Thermodynamics and Experimental Tests of Static Scaling and Universality near the Superfluid Transition in He^4 under Pressure

Guenter Ahlers
Bell Laboratories, Murray Hill, New Jersey 07974
(Received 8 November 1972)

The heat capacity at constant volume C_v and the pressure coefficient $(\partial P/\partial T)_v$ were measured near the superfluid transition on six isochores. This work also yielded new results for the derivatives $(\partial V/\partial T)_\lambda$ and $(\partial S/\partial T)_\lambda$ along the λ line (V is the molar volume and S the entropy). An essentially complete and detailed description of the thermodynamics of the superfluid transition at all pressures is provided by the data. In particular, the results were used to derive the heat capacity at constant pressure C_p, the compressibility κ, the thermal expansion coefficient α, the ratio $\gamma \equiv C_p/C_v$, and the isentropic sound velocity u, along isobars. The heat capacity C_p was examined carefully for its asymptotic behavior near T_λ. Although several interpretations of the data are possible with different assumptions about singular correction terms, it is clear that the exponents α and α' are near zero, and that the ratio A/A' of the amplitude above T_λ to the amplitude below T_λ is greater than unity and pressure dependent. The results are compared with the predictions of scaling and universality. The assumption of a pure-power-law singularity in C_v results in $\alpha \neq \alpha'$ at some pressures, and thus yields disagreement with scaling. The inclusion of singular higher-order contributions to C_p in the analysis increases the uncertainty in the exponents derived from the data, and the prediction $\alpha = \alpha'$ of scaling falls within these larger uncertainties. The amplitude ratio remains greater than unity, and thus only nonzero exponents are consistent with scaling. The pressure dependence of A/A' is not removed by the type of correction terms considered in the analysis, and is contrary to universality. When recent calculations for the exponent of the correction terms are assumed valid, then only a negative leading exponent is permitted by the data. This implies a finite C_p at T_λ. If $\alpha = \alpha' < 0$, then the data permit a continuous C_p at T_λ and at all pressures only if, contrary to universality, α and α' depend upon the pressure.

I. INTRODUCTION

In previous publications[1,2] the results of detailed measurements of the heat capacity at saturated vapor pressure C_s have been reported. Those data were compared with recent theories of critical phenomena,[3–5] and it was shown that certain simple interpretations of the results were in conflict with the Widom–Kadanoff scaling laws.[3,4] The heat-capacity measurements have now been extended to higher pressures in order to provide further data for comparison with scaling. Some of these results already have been presented briefly elsewhere.[6–8] Considerable latitude has to be allowed also in the analysis of these new data in order to obtain consistency with theory.

Near the superfluid transition, the pressure P is not a field conjugate to the order parameter. For this reason one expects the transition to remain "sharp," as P is varied. Indeed, the transition is known to exist at all pressures less than the freezing pressure (≈ 30 bar), and even the highest resolution measurements[9] show no evidence of "rounding" of the transition. Furthermore, a change in P is expected not to alter the symmetry of the order parameter. Therefore, one might expect the scaling parameters to be universal[10] in the sense that changes of an "inert" variable like P would have no effect upon them. The additional motivation for the measurements to be reported here was a desire to test this principle of universality.

The scaling predictions that will be of interest here pertain essentially to the heat capacity at constant pressure C_p. However, for P greater than the saturated vapor pressure it is experimentally inconvenient to measure C_p directly. Therefore, the heat capacity along an experimental path which was very nearly an isochore was determined; i.e., the measurements yielded approximately the heat capacity at constant volume C_v. In addition, the pressure coefficient $\partial P/\partial T$ was also measured along the same experimental path. This variable is, of course, very nearly equal to $(\partial P/\partial T)_v$. It will be demonstrated in this paper that sufficient experimental information was obtained to calculate essentially any desired thermodynamic response function, including C_p, with high precision.

The remainder of this paper is divided into several parts. In Sec. II those aspects of the experimental apparatus and procedure are described which differ from the description given previously[1] when the results at vapor pressure were presented. This section has the same structure as Sec. II of Ref. 1, and only jointly do the two publications yield a complete discussion of the experimental aspects. Section III contains some additional in-

formation about corrections to the primary data, and about probable errors in the measurements. It complements Sec. III of Ref. 1. Sections IV and V are by far the major parts of this paper. Section IV contains the primary and the derived thermodynamic results. The analysis in terms of scaling is presented in Sec. V. The reader who is not interested in the thermodynamics for its own sake, and is willing to believe that C_p can be obtained reliably from the primary data, may proceed immediately to Sec. V. Section VI is a summary of the main results of this work.

A great deal of space has been allocated in Sec. IV to a detailed discussion of the thermodynamics. This was done in part ot establish beyond any doubt the reliability of the derived results for C_p which were used in the scaling analysis. In Sec. V the data are analyzed in terms of scaling with several assumptions about higher-order contributions to C_p. Since at some time it might be desirable to make other assumptions besides the ones pursued here, the results of individual measurements are quoted in Table II.

II. EXPERIMENTAL

A. Apparatus

The apparatus used for the measurements to be reported was, except for minor modifications, the same as that described previously.[1] In this section the modifications which were necessary to facilitate work under pressure will be reported.

1. Sample-Preparation System

Figure 1 is a schematic diagram of that section of the sample preparation system which was modified for the present work, and may be compared with Fig. 1 of Ref. 1. The He^4 purification system and the gas volume measuring system (GVMS) remain unchanged. Valves labeled 1–4 are the same as those in Fig. 1 of Ref. 1. The modifications consisted of the addition of an auxiliary sample supply, a second Texas Instruments (TI) quartz-bourdon-tube pressure gauge, and a reference pressure.

The auxiliary sample supply was used only in connection with measurements on He^3-He^4 mixtures, and will not be discussed here.

The two pressure gauges were both Models 145 with micron gearing. One of them (serial No. 1344) contained a type 3 (serial No. 3880) quartz bourdon tube, had a pressure range from 0 to 0.846 bar (0–635 torr), and could be used as a differential gauge with reference pressures up to 32 bar. It is identified as LPTI in Fig. 1. The other (serial No. 1776) contained a type 1 (serial No. 3798) quartz bourdon tube, had a pressure range from 0 to 34.4 bar, and was used only as a direct reading gauge. It is identified in Fig. 1 as HPTI. It could be used either to monitor the sample pressure, or to measure the reference pressure for the LPTI gauge. At pressures less than 1 bar both gauges were calibrated as described previously.[1,11] The LPTI gauge had a resolution of 2×10^{-6} bar. For the HPTI gauge the resolution was about 10^{-4} bar. Since no facilities for calibration were available at pressures greater than 1 bar, the manufacturer's calibration was used for the HPTI gauge, and it was assumed that the sensitivity of the LPTI gauge to pressure changes was independent of the reference pressure and dependent only on the bourdon-tube deflection.

During the course of this work it became apparent that a measurable time dependence of the HPTI gauge reading existed after a rapid large He^4 gas pressure change in the bourdon tube. In order to characterize this effect, the HPTI bourdon tube was pressurized to 24 bar with He^4 gas for 20 h, and thereafter both reference and tube pressure were reduced to zero within 1 min. The gauge reading after pressure reduction is shown in Fig. 2. The relaxation effect was not troublesome for the present work because after initial pressurization large system-pressure changes generally did not occur.

The reference pressure consisted of a 3-liter volume, filled to the desired pressure with purified He^4 gas, and thermostated in a stirred water bath. A Tronac Model 1040 precision temperature controller was used to maintain the water bath at constant temperature. With constant pressure applied to the bourdon tube of the LPTI gauge[12] and the reference pressure connected to the reference port of the same gauge, it was established that the

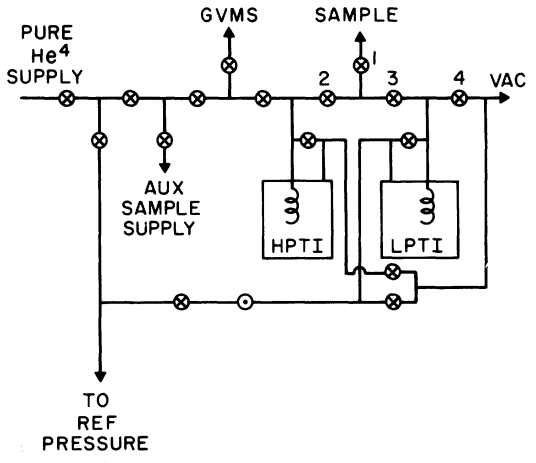

FIG. 1. Schematic diagram of the sample preparation system.

reference pressure had a short-term (≈ 1 h) stability of 1 ppm. Long-term drifts were not detectable with the HPTI gauge. One ppm stability in the pressure corresponds to a thermal stability of the controlled bath of 3×10^{-4} °C.

2. Calorimeter

Minor changes from the original design[1] were made in this system after the measurements with P_λ equal to vapor pressure, 1.65 bar, and 15.03 bar were completed.

The length of the probe was reduced from 0.95 cm to 0.09 cm. Whereas prior to this modification the probe volume was 1% of the total sample volume, the probe contained only 0.1% of the sample after the change. Thermal relaxation times in the short probe when filled with He I were less than 1 min, and thermal gradients could be kept extremely small. Nonetheless, sufficient sensitivity for the detection of T_λ was maintained, and the transition temperature could still be measured to $\pm10^{-7}$ K.

An auxiliary capillary was added to the system. The bottom end of this capillary was thermally attached to, but did not connect with, the sample volume. When helium was introduced to this capillary, it served as an additional superfluid heat leak for cooling the system. When this helium was removed, virtually perfect thermal isolation was still attainable. The addition of this capillary made it possible to cool the sample without appreciably disturbing the thermal gradients in the main capillary.[13,14]

The heat leaks from the cell to the isothermal platform and from the isothermal platform to the bath were increased to 10^{-5} and 10^{-4} W/K, respectively. This was done to permit certain other experiments[15] which will not be discussed here, and which required greater power dissipation in the sample than had been possible with the previous design. Even after this modification, conduction-heat leaks were more stable than parasitic power inputs, and the thermal stability of the apparatus was as reported previously.[1]

B. Thermometer Calibration

The thermometer was calibrated against the sample vapor pressure before the sample chamber had been completely filled, as described previously.[1] It was discovered, however, that pressurizing the sample chamber subjected the thermometer to sufficient strains to slightly change its calibration. This was the case even though the thermometer was mounted on the outside of the heavy walled sample container and must have been caused by the elastic deformation of this container. Less precise calibrations against the bath vapor pressure, using exchange gas in the main vacuum, indicated, however, that shifts of the thermometer calibration due to the sample pressure did not exceed 3×10^{-3} K, and that systematic errors in C_v and $(\partial P/\partial T)_v$ due to uncertainties from this source in the temperature scale did not exceed 1%. The resulting relative errors in a set of data at a given density are of course constant, and scaling parameters (see Sec. V) such as α, α', and A/A' are not affected.

C. Procedure

In addition to C_v, it was desired to measure simultaneously also the pressure coefficient $(\partial P/\partial T)_v$. This was accomplished by adjusting the reference pressure of the LPTI gauge to a value slightly less than the sample pressure, and by leaving valves 1 and 3 (Fig. 1) open, thus connecting the LPTI gauge to the sample. Under these conditions, there is a small system volume at room temperature (3.5 cm^3) connected to the sample volume, and appropriate corrections (see Sec. III A) have to be applied. By means of the LPTI gauge, the sample pressure change resulting from the same temperature change used for the determination of a heat-capacity point could be determined. Otherwise, the procedure was rather similar to that described for the measurements at vapor pressure.[1]

D. Performance

The general performance of the apparatus was described previously[1] and only those aspects peculiar to the measurements under pressure will be discussed here.

1. Thermal Stability

When the sample was superfluid, its thermal stability was not as great during the C_v measurements as it was at saturated vapor pressure. Typical sample temperature drift rates were given in Table II of Ref. 1. Nonetheless, for $T_\lambda - T \lesssim 10^{-2}$ K, it was possible to make measurements nearly

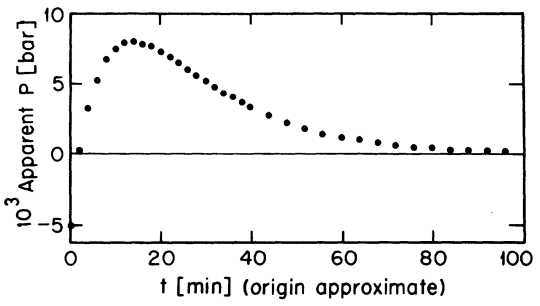

FIG. 2. Apparent pressure indicated by the HPTI gauge with zero applied pressure, after pressurization of the bourdon tube to 24 bar with He^4 gas for 20 h.

as precise as at vapor pressure. For $T > T_\lambda$, the system functioned as well during the C_v measurements as it did at saturated vapor pressure.

2. *Constancy of Sample Mass*

During the measurements of C_s, there was no reason for any appreciable change in the sample mass. During the measurements of C_v and $(\partial P/\partial T)_v$, however, the sample mass could have changed for two reasons. A time dependence of the temperature gradient in the capillary would result in a change of the distribution of the helium between the capillary and the sample chamber. As pointed out in Ref. 1, this effect was minimized by controlling the thermal gradient in the capillary, and by establising a large temperature gradient immediately above the point where the capillary entered the main vacuum (see Fig. 2 of Ref. 1). In addition, a continuous loss of sample had to be expected when the quartz-bourdon-tube gauge was used to monitor the sample pressure because of diffusion of helium through the quartz. In order to establish experimentally the magnitude of this sample loss, the transition pressure P_λ near 2.15 K was determined several times over a two-hour period with a 1.6-bar pressure differential across the bourdon tube. The results are shown in Fig. 3. The transition pressure dropped at a rate of 9×10^{-7} bar/min, corresponding to a transition temperature change of 9×10^{-9} K/min. The change in T_λ was too small to be separated experimentally from the time dependence of the thermometer resistance.[1] From the time dependence of P_λ it can be estimated that the rate of change of the sample mass was 3.4×10^{-8} mole/min, or 0.011 ppm/min. Clearly this is insignificant provided that the time dependence of T_λ is determined and considered in the data analysis. It corresponds to a helium diffusion rate through the quartz bourdon tube of 1.0×10^{-8} cm^3/sec torr D, which is within the pressure-gauge manufacturer's specification. Independent measurements of this diffusion rate yielded 1.2×10^{-8} cm^3/sec torr D, indicating that the change in sample mass deduced from P_λ was indeed caused primarily by diffusion through the bourdon tube. The scatter of P_λ about the straight line in Fig. 3 is about $\pm2\times10^{-6}$ bar or 1 ppm of P_λ. This is in agreement with the expected resolution of the pressure gauge. The results indicate that any sample redistribution due to changes in the temperature gradient in the capillary was negligible.

III. DATA ANALYSIS

A. Corrections

The curvature correction discussed in Ref. 1 was applied to all data.

The measurements have been corrected for the effect of gravity[16] which was discussed extensively in Ref. 1. Since none of the present measurements are extremely near T_λ, this effect is small, and we thought it preferable to correct the measurements to zero gravity. At vapor pressure, where measurements were made for which the effect was large, the data had not been corrected, and instead were fitted to functions which included the gravity effect.[1]

The experimental measurements designed to yield C_v and $(\partial P/\partial T)_v$ do not give these quantities directly. The small quantity of gas at room temperature (about 3.5 cm^3; see also Sec. II C and Table I of Ref. 1) is compressible, and the pressure changes associated with sample temperature changes cause flow along the capillary, and result in a small dependence of the molar volume V of the liquid upon the temperature. Thus, for instance, the quantity measured is not $C_v \equiv T(\partial S/\partial T)_v$, but rather $C_x \equiv T(\partial S/\partial T)_x$, where x indicates the experimental path. However, it can be shown that

$$C_x - C_v = T(\partial P/\partial T)_v\,(\partial V/\partial T)_x\ . \tag{3.1}$$

Using the relation

$$(\partial P/\partial T)_v = (\partial S/\partial V)_t - T^{-1}C_v(\partial T/\partial V)_t \tag{3.2}$$

where $t \equiv T - T_\lambda$, one obtains

$$C_v = \frac{C_x - T(\partial S/\partial V)_t(\partial V/\partial T)_x}{1 - (\partial T/\partial V)_t\,(\partial V/\partial T)_x}\ . \tag{3.3}$$

Near T_λ, $(\partial S/\partial V)_t$ and $(\partial T/\partial V)_t$ may for the present purpose (see also Secs. IV C and IV D) be approximated by $(\partial S/\partial V)_\lambda$ and $(\partial T/\partial V)_\lambda$. For the change in molar volume of the liquid along the experimental path one has

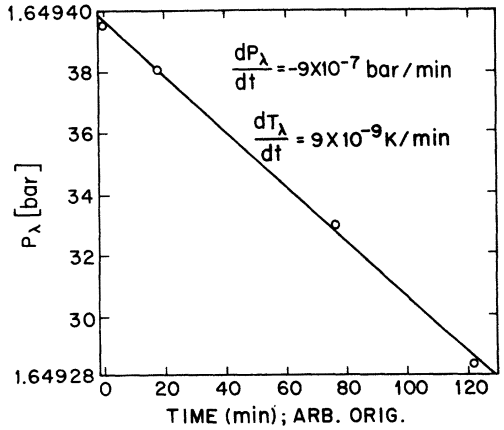

FIG. 3. Time dependence of P_λ. This effect is caused by the sample loss due to He^4 gas diffusion through the quartz bourdon tube used to monitor P_λ.

$$\left(\frac{\partial V}{\partial T}\right)_x = \frac{V_c R T_R V_R}{(nRT_R - PV_R)^2}\left(\frac{\partial P}{\partial T}\right)_x \qquad (3.4)$$

if the vapor can be treated as an ideal gas. Here T_R is the room temperature, V_R the volume at T_R, n the total number of moles of sample, V_c the volume of the sample chamber, and R the gas constant. Evaluation of C_v from the measured C_x and $(\partial P/\partial T)_x$, and from the known volumes of the system, revealed that C_v never differed from C_x by more than 0.3% over the temperature and pressure range of interest. A sufficiently accurate correction for this effect therefore could be applied.

There are two additional effects which at least in principle should be considered. During the C_v measurements the number of moles of helium in the sample chamber is temperature dependent because of the pressure change in the room-temperature volume. However, the ratio between the number of moles of helium at room temperature and that in the cell is no greater than 10^{-3} at the pressures used in this experiment, and changes by less than 10^{-4} because of pressure changes along an "isochore." Thus the amount of sample used for the measurement may be regarded as constant. The second effect is a consequence of the negative thermal-expansion coefficient of liquid helium in the temperature range of interest. As the sample temperature is increased, additional material *enters* the calorimeter, and this additional material, although it has a negligible effect on the total amount of sample, introduces energy into the system because it is approximately at a temperature $T' > T$. However, it can be estimated that under the experimental conditions used here the resulting error in C_x is always less than one part in 10^4.

For the pressure coefficient, a correction similar to Eq. (3.3) for C_v applies, and is given by

$$\left(\frac{\partial P}{\partial T}\right)_v = \frac{(\partial P/\partial T)_x - (\partial V/\partial T)_x(\partial P/\partial V)_t}{1 - (\partial V/\partial T)_x(\partial T/\partial V)_t} \quad . \qquad (3.5)$$

The difference between $(\partial P/\partial T)_v$ and $(\partial P/\partial T)_x$ never exceeds 0.8% of $(\partial P/\partial T)_v$ over the temperature and pressure range of interest, and a correction is readily applied.

B. Errors

The discussion in Ref. 1 of errors at vapor pressure is applicable to the present results for C_v, except that random errors for He II are perhaps slightly larger because of the larger sample temperature drifts (Table II of Ref. 1). Since it was desirable to make measurements at several volumes, fewer data could be obtained at any one volume in a reasonable length of time than at saturated vapor pressure.[1] Primarily for this reason, the random errors for derived parameters such as the exponents α and α' or amplitudes A_0 and A_0' (see Sec. V) are in most cases slightly larger than they were at vapor pressure. We already discussed (Sec. II B) the larger uncertainty in the temperature scale for the present work. Systematic errors in addition to those discussed in Ref. 1 of about 1% which may be different at different densities must be expected from this source.

The random errors in $(\partial P/\partial T)_v$ are determined by the pressure resolution, and are estimated to be about 1% of $(\partial P/\partial T)_v$. Systematic errors of about 1% due to possible systematic errors in the pressure scale[1] may also apply to this variable.

IV. RESULTS

A. Heat Capacity at Constant Volume

Measurements of C_v were made along six isochores. The molar volumes and corresponding temperatures and pressures at the λ point are listed in Table I. Of the entries in Table I, the pressure P_λ was measured directly, and T_λ and V_λ are derived from the equations given by Kierstead.[17] Direct determinations of T_λ, although they differ from those given in Table I by not more than 2×10^{-3} K, are considered less reliable because of the effect of the sample pressure on the temperature scale which was discussed in Secs. II B and III B. No direct determination of the molar volume was made. The results of individual measurements along each isochore are listed in Table II, and some of the results have already been shown in Fig. 2 of Ref. 6 as a function of $\log_{10}|T_\lambda - T|$.

It is well known that C_v is finite at T_λ.[18] Nonetheless, the data in Fig. 2 of Ref. 6 suggest that the function

$$C_v = -A_{0v}\ln|t| + B_{0vt}, \quad t \equiv T - T_\lambda(V) \qquad (4.1)$$

which diverges at T_λ, is a good approximation to the experimental results over a considerable range in t. We have fitted the data with $10^{-4}\,\mathrm{K} \le |t| \le 3\times10^{-3}\,\mathrm{K}$ for each phase along each isochore separately to Eq. (4.1), and list the resulting coefficients in Table III. Here, a distinction between

TABLE I. Parameters for the λ points on the experimental isochores.

P_λ (bar)	T_λ (K)	V_λ ($cm^3 mole^{-1}$)
1.646	2.157	26.81
7.328	2.095	25.31
15.031	1.998	23.95
18.180	1.954	23.51
22.533	1.889	22.97
25.868	1.836	22.60

TABLE II. Results of individual measurements of the heat capacity and the pressure coefficient.

$10^3[T-T_\lambda(V)]$ (K)	C_v (J mole^{-1} K^{-1})	$(\partial P/\partial T)_v$ (bar K^{-1})	$10^3[T-T_\lambda(P)]$ (K)	C_p (J mole^{-1} K^{-1})
		$P_\lambda=1.65$ bar		
0.4990	35.85	−2.438	0.4843	36.25
1.268	31.03	−1.717	1.239	31.24
2.078	28.41	−1.334	2.037	28.53
2.954	26.54	−1.083	2.902	26.62
5.112	23.72	−0.6893	5.042	23.74
8.045	21.37	−0.3195	7.959	21.37
9.499	20.55	−0.2007	9.408	20.55
11.13	19.74	−0.0821	11.04	19.74
12.55	19.15	0.0101	12.45	19.14
16.83	17.77	0.2287	16.73	17.77
0.5870	35.01	−2.203	0.5703	35.37
0.7985	33.33	−1.994	0.7775	33.62
0.9462	32.58	−1.854	0.9224	32.84
1.147	31.50	−1.737	1.120	31.72
1.455	30.25	−1.574	1.423	30.43
−23.35	36.46	−2.652	−22.62	37.02
−21.70	36.93	−2.681	−21.01	37.50
−20.09	37.33	−2.735	−19.44	37.92
−18.49	37.77	−2.822	−17.89	38.38
−16.87	38.30	−2.899	−16.31	38.93
−15.23	38.83	−2.934	−14.71	39.49
−13.60	39.43	−2.989	−13.13	40.11
−11.98	40.14	−3.075	−11.56	40.85
−10.36	40.94	−3.175	−9.984	41.69
−8.717	41.78	−3.279	−8.391	42.59
−7.088	42.83	−3.442	−6.814	43.69
−5.949	43.66	−3.549	−5.713	44.58
−5.294	44.16	−3.618	−5.080	45.11
−4.639	44.97	−3.689	−4.447	45.97
−3.977	45.62	−3.755	−3.809	46.67
−3.328	46.50	−3.874	−3.184	47.61
−2.663	47.58	−3.999	−2.544	48.77
−2.173	48.64	−4.115	−2.073	49.91
−1.861	49.27	−4.193	−1.774	50.60
−1.531	50.16	−4.351	−1.457	51.56
−1.205	51.34	−4.456	−1.145	52.85
−0.8784	52.66	−4.666	−0.8331	54.29
−0.5516	54.84	−4.953	−0.5215	56.69
−0.2231	59.02	−5.592	−0.2097	61.33
−1.136	51.62	−4.582	−1.079	53.16
−1.031	51.97	−4.612	−0.9788	53.54
−0.9263	52.47	−4.660	−0.8788	54.08
−0.8225	53.25	−4.756	−0.7797	54.94
−0.7165	53.60	−4.793	−0.6786	55.32
−0.6154	54.35	−4.871	−0.5823	56.15
−0.4204	56.21	−5.168	−0.3968	58.21
−0.3213	57.18	−5.264	−0.3027	59.28
−0.2224	59.21	−5.575	−0.2090	61.53
−0.1529	61.16	−5.788	−0.1433	63.72
−0.1210	62.13	−5.957	−0.1133	64.82
−0.0888	63.07	−6.127	−0.0829	65.87
−0.0527	65.93	−6.515	−0.0491	69.11
−0.0363	67.07	−6.516	−0.0337	70.41
		$P_\lambda=7.33$ bar		
−10.55	36.27	−6.563	−9.609	38.42
−10.16	36.42	−6.548	−9.255	38.59
−9.406	36.85	−6.809	−8.556	39.09

TABLE II. (*Continued*)

$10^3[T-T_\lambda(V)]$ (K)	C_v (J mole^{-1} K^{-1})	$(\partial P/\partial T)_v$ (bar K^{-1})	$10^3[T-T_\lambda(P)]$ (K)	C_p (J mole^{-1} K^{-1})
		$P_\lambda = 7.33$ bar		
−9.037	36.95	−6.775	−8.216	39.20
−8.375	37.33	−6.844	−7.607	39.64
−7.998	37.58	−6.859	−7.261	39.94
−7.653	37.71	−6.854	−6.943	40.08
−7.304	37.92	−7.005	−6.623	40.32
−6.971	38.13	−6.939	−6.317	40.57
−6.618	38.38	−6.994	−5.993	40.86
−6.279	38.54	−7.149	−5.682	41.05
−5.921	38.84	−7.132	−5.354	41.39
−5.587	39.10	−7.155	−5.048	41.70
−5.241	39.30	−7.337	−4.732	41.94
−4.910	39.62	−7.394	−4.429	42.32
−4.577	39.85	−7.428	−4.125	42.59
−4.238	40.19	−7.601	−3.816	42.99
−3.908	40.47	−7.605	−3.514	43.32
−3.573	40.89	−7.616	−3.210	43.83
−3.247	41.31	−7.813	−2.913	44.32
−2.913	41.70	−7.820	−2.610	44.80
−2.589	42.21	−7.849	−2.316	45.40
−2.265	42.73	−8.069	−2.023	46.03
−1.945	43.35	−8.225	−1.733	46.79
−1.626	44.04	−8.362	−1.446	47.63
−1.306	44.91	−8.597	−1.157	48.70
−0.9869	45.98	−8.937	−0.8716	50.02
−0.6739	47.40	−9.363	−0.5922	51.79
−0.3607	49.86	−10.09	−0.3143	54.91
0.1400	36.96	−6.593	0.1271	39.08
0.2345	34.94	−6.015	0.2146	36.73
0.3837	32.69	−5.425	0.3537	34.14
0.5823	30.77	−4.979	0.5401	31.95
0.7739	29.41	−4.641	0.7208	30.43
0.9569	28.46	−4.407	0.8941	29.36
1.211	27.40	−4.107	1.135	28.19
1.537	26.21	−3.827	1.446	26.88
1.858	25.41	−3.591	1.753	26.01
2.175	24.65	−3.343	2.057	25.18
2.496	24.03	−3.193	2.365	24.50
2.814	23.43	−3.082	2.672	23.86
−0.7394	47.22	−9.379	−0.6505	51.57
−0.6413	47.76	−9.615	−0.5631	52.25
−0.5471	48.36	−9.711	−0.4794	53.01
−0.4532	48.94	−9.697	−0.3961	53.75
−0.3577	49.98	−9.929	−0.3117	55.07
−0.3472	50.12		−0.3024	55.25
−0.2476	51.34		−0.2147	56.82
−0.1517	53.19		−0.1307	59.22
0.1058	38.33		0.0957	40.70
		$P_\lambda = 15.03$ bar		
−5.047	33.97	−12.10	−4.132	39.22
−4.721	34.22	−12.15	−3.860	39.56
−4.401	34.43	−12.32	−3.592	39.85
−4.077	34.69	−12.52	−3.323	40.23
−3.759	34.93	−12.73	−3.058	40.57
−3.433	35.13	−12.45	−2.787	40.84
−2.990	35.68	−12.75	−2.420	41.65
−2.676	35.97	−12.94	−2.160	42.06
−1.487	37.84	−13.96	−1.185	44.82
−1.334	38.15	−13.92	−1.061	45.27

TABLE II. (*Continued*)

$10^3[T-T_\lambda(V)]$ (K)	C_v (J mole^{-1} K^{-1})	$(\partial P/\partial T)_v$ (bar K^{-1})	$10^3[T-T_\lambda(P)]$ (K)	C_ϕ (J mole^{-1} K^{-1})
		$P_\lambda = 15.03$ bar		
−1.169	38.58	−14.10	−0.9263	45.93
−1.008	38.99	−14.18	−0.7962	46.55
−0.8436	39.55	−14.56	−0.6636	47.41
−0.6898	40.16	−14.71	−0.5402	48.36
−0.5405	40.78	−14.98	−0.4209	49.33
−0.4017	41.70	−15.39	−0.3106	50.80
−0.2621	42.89	−16.02	−0.2007	52.71
−0.1160	45.08	−17.05	−0.0871	56.34
0.1884	30.56	−10.53	0.1573	34.34
0.3725	28.01	−9.251	0.3170	30.95
0.5534	26.53	−8.528	0.4764	29.03
0.7262	25.46	−7.953	0.6299	27.66
0.9019	24.57	−7.774	0.7871	26.54
1.141	23.55	−7.305	1.002	25.27
1.439	22.59	−6.810	1.272	24.10
1.734	21.86	−6.455	1.541	23.22
2.176	20.92	−6.074	1.945	22.09
2.764	19.94	−5.484	2.487	20.93
3.348	19.10	−5.175	3.028	19.95
−0.4083	41.68	−15.68	−0.3159	50.76
−0.3071	42.57	−15.66	−0.2360	52.19
−0.2186	43.57	−16.34	−0.1667	53.83
−0.1296	45.03	−16.82	−0.0976	56.25
−0.0467	47.59	−18.26	−0.0343	60.66
0.0549	34.82	−12.63	0.0442	40.31
0.1485	31.35	−10.85	0.1231	35.42
0.3638	28.04	−9.310	0.3095	30.98
		$P_\lambda = 18.18$ bar		
−3.416	32.86	−14.54	−2.634	39.85
−3.091	33.17	−14.57	−2.378	40.32
−2.768	33.46	−14.66	−2.123	40.79
−2.415	33.82	−14.94	−1.845	41.35
−2.114	34.16	−15.16	−1.610	41.91
−1.819	34.62	−15.58	−1.380	42.66
−1.518	35.07	−15.86	−1.145	43.40
−1.222	35.59	−15.90	−0.9173	44.26
−0.9879	36.29	−16.22	−0.7371	45.43
−0.8377	36.66	−16.34	−0.6223	46.06
−0.6881	37.15	−16.60	−0.5084	46.91
−0.5376	37.80	−17.29	−0.3945	48.05
−0.3889	38.48	−17.45	−0.2828	49.24
−0.2426	39.74	−18.10	−0.1741	51.52
−0.0996	41.85	−19.51	−0.0697	55.47
−0.7038	37.17	−16.69	−0.5203	46.93
−0.6170	37.42	−16.67	−0.4545	47.37
−0.5308	37.84	−17.24	−0.3894	48.10
−0.4425	38.24	−17.24	−0.3229	48.82
−0.3538	38.78	−17.42	−0.2566	49.78
−0.1774	40.55	−18.64	−0.1262	53.01
−0.0890	42.10	−19.47	−0.0621	55.95
−0.2773	39.50	−18.02	−0.1998	51.07
−0.1894	40.29	−18.65	−0.1350	52.54
−0.1056	41.77	−19.16	−0.0740	55.33
−0.3036	39.14	−17.97	−0.2193	50.43
−0.2126	39.99	−18.20	−0.1520	51.97
−0.1249	41.29	−19.59	−0.0880	54.40
−5.366	31.58	−14.03	−4.187	37.86
−4.777	31.91	−14.03	−3.716	38.38

TABLE II. (*Continued*)

$10^3[T-T_\lambda(V)]$ (K)	C_v (J mole^{-1} K^{-1})	$(\partial P/\partial T)_v$ (bar K^{-1})	$10^3[T-T_\lambda(P)]$ (K)	C_p (J mole^{-1} K^{-1})
		$P_\lambda = 18.18$ bar		
−4.186	32.26	−14.15	−3.245	38.90
−3.606	32.71	−14.43	−2.785	39.60
−3.039	33.17	−14.82	−2.337	40.32
−2.571	33.66	−15.08	−1.968	41.10
−2.279	34.02	−15.15	−1.738	41.68
−1.986	34.37	−15.31	−1.510	42.25
−1.692	34.81	−15.57	−1.281	42.96
−1.398	35.29	−15.73	−1.053	43.75
−1.104	35.91	−16.21	−0.8259	44.79
−0.8098	36.74	−16.87	−0.6009	46.20
−0.5160	37.87	−17.43	−0.3782	48.16
−0.1917	40.27	−18.63	−0.1367	52.49
0.0653	32.21	−14.12	0.0500	38.70
0.1519	29.39	−12.64	0.1202	34.39
0.2456	27.59	−11.43	0.1979	31.75
0.3406	26.49	−10.51	0.2776	30.20
0.0451	33.24	−14.59	0.0341	40.35
0.1249	29.98	−12.83	0.0981	35.28
0.2100	27.85	−11.99	0.1682	32.14
0.2998	26.81	−11.06	0.2433	30.64
0.0856	31.16	−13.81	0.0663	37.07
0.2319	27.70	−11.74	0.1864	31.91
0.3794	25.93	−10.67	0.3104	29.41
0.5280	24.72	−9.990	0.4371	27.75
0.6790	23.87	−9.388	0.5671	26.59
0.8322	23.09	−8.894	0.7000	25.55
0.9857	22.41	−8.595	0.8341	24.66
1.212	21.64	−8.222	1.033	23.65
1.504	20.81	−7.711	1.291	22.59
1.797	20.10	−7.311	1.552	21.70
2.102	19.47	−7.094	1.825	20.91
2.403	18.96	−6.673	2.096	20.28
2.854	18.35	−6.338	2.504	19.53
3.445	17.62	−6.020	3.042	18.64
4.023	17.00	−5.636	3.570	17.89
4.922	16.23	−5.266	4.397	16.99
6.179	15.36	−5.155	5.561	15.97
7.500	14.63	−4.259	6.793	15.13
8.885	14.00	−3.896	8.092	14.41
12.71	12.72	−3.198	11.71	12.97
19.37	11.20	−2.283	18.08	11.31
26.78	10.24	−1.680	25.26	10.27
34.88	9.399	−1.147	33.17	9.385
		$P_\lambda = 22.53$ bar		
−5.957	28.58	−16.24	−4.327	36.16
−5.615	28.73	−16.50	−4.071	36.42
−5.318	28.83	−16.46	−3.849	36.58
−5.007	29.04	−16.44	−3.617	36.96
−4.700	29.19	−16.38	−3.389	37.22
−4.411	29.37	−16.56	−3.173	37.54
−4.102	29.48	−16.73	−2.944	37.74
−3.803	29.67	−16.99	−2.723	38.08
−3.508	29.86	−17.24	−2.505	38.42
−3.195	30.03	−17.26	−2.275	38.71
−2.731	30.44	−17.36	−1.935	39.46
−2.442	30.63	−17.42	−1.723	39.80
−2.151	30.94	−17.63	−1.512	40.39

TABLE II. (*Continued*)

$10^3[T-T_\lambda(V)]$ (K)	C_v (J mole^{-1} K^{-1})	$(\partial P/\partial T)_v$ (bar K^{-1})	$10^3[T-T_\lambda(P)]$ (K)	C_p (J mole^{-1} K^{-1})
		$P_\lambda = 22.53$ bar		
−1.857	31.28	−18.03	−1.299	41.03
−1.567	31.62	−18.40	−1.090	41.68
−1.338	31.94	−18.83	−0.9261	42.28
−1.246	32.21	−18.78	−0.8601	42.82
−1.155	32.33	−19.05	−0.7952	43.05
−1.065	32.54	−18.98	−0.7315	43.45
−0.9766	32.68	−18.86	−0.6687	43.74
−0.7972	33.03	−19.28	−0.5421	44.42
−0.7103	33.32	−19.40	−0.4811	45.00
−0.6239	33.57	−19.63	−0.4207	45.52
−0.5377	33.82	−19.40	−0.3607	46.03
−0.4516	34.17	−20.08	−0.3012	46.76
−0.3673	34.59	−20.12	−0.2432	47.63
−0.1208	36.76	−21.44	−0.0769	52.38
−0.0422	38.58	−23.39	−0.0259	56.63
0.0415	30.57	−17.76	0.0286	39.61
0.1223	27.22	−14.96	0.0891	33.64
0.2124	25.53	−13.77	0.1590	30.84
0.4065	23.28	−12.40	0.3143	27.31
0.7215	21.37	−10.99	0.5733	24.47
1.023	20.16	−9.939	0.8267	22.74
1.308	19.32	−9.447	1.069	21.58
1.588	18.67	−8.870	1.309	20.69
2.005	17.82	−8.361	1.670	19.56
2.581	16.92	−7.684	2.174	18.38
−0.3724	34.66	−19.98	−0.2467	47.79
−0.2857	35.04	−20.21	−0.1875	48.58
0.0418	30.45	−17.09	0.0287	39.39
0.1127	27.49	−15.23	0.0817	34.09
		$P_\lambda = 25.86$ bar		
−30.63	22.88	−16.07	−21.74	29.09
−29.20	23.04	−16.05	−20.69	29.38
−27.66	23.25	−16.17	−19.56	29.75
−26.21	23.38	−16.37	−18.50	29.96
−24.68	23.52	−16.44	−17.38	30.20
−23.25	23.69	−16.43	−16.34	30.51
−21.83	23.90	−16.69	−15.31	30.87
−20.35	24.05	−16.79	−14.23	31.14
−17.47	24.44	−16.98	−12.15	31.83
−15.96	24.66	−17.18	−11.07	32.24
−14.52	24.93	−17.37	−10.03	32.73
−13.11	25.13	−17.47	−9.024	33.11
−11.71	25.40	−17.74	−8.026	33.61
−10.31	25.67	−17.94	−7.034	34.12
−8.936	25.98	−18.16	−6.064	34.72
−7.569	26.30	−18.30	−5.104	35.33
−6.426	26.70	−18.76	−4.306	36.13
−5.854	26.82	−18.61	−3.909	36.36
−5.283	27.06	−18.87	−3.514	36.85
−4.719	27.30	−19.30	−3.126	37.33
−4.159	27.49	−19.10	−2.741	37.73
−2.429	28.56	−19.94	−1.568	40.00
−4.782	27.30	−19.28	−3.169	37.34
−4.204	27.52	−19.13	−2.772	37.80
−3.653	27.80	−19.38	−2.395	38.38
−3.098	28.18	−19.85	−2.019	39.19
−2.547	28.54	−19.94	−1.647	39.97

TABLE II. (*Continued*)

$10^3[T-T_\lambda(V)]$ (K)	C_v (J mole^{-1} K^{-1})	$(\partial P/\partial T)_v$ (bar K^{-1})	$10^3[T-T_\lambda(P)]$ (K)	C_p (J mole^{-1} K^{-1})
		$P_\lambda = 25.86$ bar		
−1.996	29.01	−20.32	−1.279	41.00
−1.445	29.56	−21.07	−0.9136	42.25
−0.8942	30.50	−21.57	−0.5544	44.45
−0.3716	32.06	−23.05	−0.2222	48.31
−5.367	26.98	−18.58	−3.572	36.68
−5.087	27.08	−18.49	−3.379	36.89
−4.806	27.30	−18.80	−3.185	37.34
−4.526	27.37	−18.97	−2.993	37.49
−4.246	27.50	−19.09	−2.801	37.75
−3.968	27.62	−19.19	−2.610	38.00
−3.691	27.80	−19.23	−2.422	38.38
−3.416	27.96	−19.28	−2.234	38.73
−3.144	28.05	−19.31	−2.050	38.90
−2.866	28.24	−19.59	−1.862	39.31
−2.598	28.48	−19.89	−1.682	39.85
−2.324	28.64	−20.10	−1.497	40.19
−2.044	28.85	−20.06	−1.311	40.65
−1.769	29.19	−20.37	−1.128	41.41
−1.494	29.40	−20.37	−0.9456	41.89
−1.219	29.91	−20.69	−0.7654	43.05
−0.9436	30.41	−21.42	−0.5864	44.23
−0.6664	30.89	−22.09	−0.4083	45.40
−0.3913	31.88	−22.65	−0.2344	47.87
−1.298	29.80	−20.73	−0.8173	42.80
−1.081	30.05	−21.02	−0.6757	43.39
−0.7947	30.77	−21.66	−0.4904	45.10
−0.6532	31.05	−21.78	−0.3998	45.79
−0.5158	31.43	−22.19	−0.3126	46.72
−0.3792	31.94	−22.83	−0.2269	48.03
−0.2419	32.71	−23.54	−0.1420	50.02
−0.1275	33.67	−24.54	−0.0727	52.64
−0.5782	31.31	−22.16	−0.3521	46.43
−0.4372	31.76	−22.42	−0.2631	47.56
−0.2982	32.42	−23.26	−0.1766	49.27
−0.1584	33.36	−24.12	−0.0913	51.78
−0.3573	32.13	−22.22	−0.2133	48.52
−0.2175	32.94	−23.72	−0.1270	50.63
−0.0794	34.44	−24.35	−0.0443	54.82
−0.6081	31.19	−22.19	−0.3711	46.12
−0.4686	31.66	−22.63	−0.2829	47.30
−0.3291	32.28	−23.00	−0.1957	48.89
−0.1901	33.16	−23.36	−0.1104	51.22
−0.0694	34.66	−25.15	−0.0386	55.45
0.0603	27.24	−18.89	0.0383	37.06
0.1726	24.20	−16.04	0.1181	31.05
0.3133	22.46	−14.59	0.2228	27.92
0.0775	26.66	−18.32	0.0502	35.86
0.2054	23.76	−15.64	0.1421	30.25
0.3450	22.24	−14.38	0.2469	27.54
0.0876	26.18	−18.10	0.0572	34.89
0.2237	23.55	−15.43	0.1557	29.86
0.3601	22.02	−14.33	0.2584	27.16
0.4976	21.08	−13.54	0.3644	25.58
0.6351	20.29	−12.94	0.4721	24.29
0.7739	19.70	−12.35	0.5823	23.35
0.9136	19.14	−11.60	0.6943	22.48

TABLE II. *(Continued)*

$10^3[T-T_\lambda(V)]$ (K)	C_v (J mole^{-1} K^{-1})	$(\partial P/\partial T)_v$ (bar K^{-1})	$10^3[T-T_\lambda(P)]$ (K)	C_p (J mole^{-1} K^{-1})
		$P_\lambda = 25.86$ bar		
1.052	18.70	−11.70	0.8064	21.79
1.258	18.09	−10.84	0.9740	20.88
1.534	17.42	−10.28	1.202	19.88
1.813	16.85	−9.751	1.435	19.06
2.093	16.39	−9.267	1.670	18.41
2.372	15.95	−8.962	1.906	17.80
2.789	15.41	−8.500	2.262	17.06
3.348	14.79	−8.053	2.742	16.21
4.032	14.16	−7.554	3.337	15.38
4.858	13.54	−6.962	4.062	14.57
6.177	12.74	−6.240	5.233	13.56
8.036	11.89	−5.499	6.904	12.50
−0.2588	32.69		−0.1523	49.99
−0.2307	32.87		−0.1351	50.46
−0.2020	33.12		−0.1177	51.14
−0.1732	33.32		−0.1002	51.68
−0.0594	34.82		−0.0327	55.92
−0.0348	35.63		−0.0187	58.35
0.0306	28.32		0.0185	39.39
0.0609	26.76		0.0388	36.08
0.4133	21.59		0.2992	26.43
0.6727	20.15		0.5019	24.06
1.197	18.26		0.9247	21.12
2.340	16.02		1.879	17.89
5.020	13.45		4.205	14.45
9.113	11.49		7.881	12.02
13.83	10.19		12.22	10.48
19.08	9.243		17.15	9.394
24.82	8.509		22.60	8.574

the two phases is made by using primed coefficients for the low-temperature phase (He II). It is possible to represent the coefficients in Table III by smooth functions of P_λ, V_λ, or T_λ. We have chosen to write them as functions of P_λ, and obtained

$$\begin{aligned} A'_{0v} &= 4.909(1 - 0.03060P_\lambda + 0.0002343P_\lambda^2)\,, \\ B'_{0vt} &= 20.00(1 - 0.00425P_\lambda)\,, \\ A_{0v} &= 5.252(1 - 0.01903P_\lambda + 0.0001578P_\lambda^2)\,, \\ B_{0vt} &= -3.00(1 + 0.00595P_\lambda) \end{aligned} \tag{4.2}$$

from a least-squares fit involving all data with $10^{-4} \leq |t| \leq 3\times10^{-3}$ K. The units of C_v are in J mole^{-1}K^{-1}, and $P_\lambda(V)$ is the pressure in bars at $T_\lambda(V)$ on the isochore with volume V. In order to determine how well Eq. (4.1) with the coefficients given by Eq. (4.2) represents the measurements, in Fig. 4 we show in percent the deviations from Eqs. (4.1) and (4.2) of the individual data points. It can be seen that all the data for which $10^{-4} \leq |t| \leq 5\times10^{-3}$ K deviate from Eqs. (4.1) and (4.2) by no more than 1%. It is clear that the relatively simple form of Eqs. (4.1) and (4.2) may be used for many not too demanding thermodynamic calculations.

For some purposes it is more convenient to consider the specific heat as a function of the reduced temperature interval $\epsilon_t \equiv t/T_\lambda$, i.e.,

$$C_v = -A_{0v}\ln|\epsilon_t| + B_{0v}\,. \tag{4.3}$$

It is apparent that this choice of variables does not alter A_{0v}. However,

$$B_{0v} = B_{0vt} - A_{0v}\ln T_\lambda\,. \tag{4.4}$$

The values of B_{0v} are also listed in Table III, and

TABLE III. Least-squares parameters for C_v on the experimental isochores. See Eqs. (4.1) and (4.3). C_v in J mole^{-1}K^{-1}.

P_λ	A_{ov}	B_{ovt}	B_{ov}	A'_{ov}	B'_{ovt}	B'_{ov}
1.646	5.062	−2.82	−6.71	4.612	20.29	16.74
7.328	4.563	−3.30	−6.67	3.890	19.06	16.18
15.031	3.940	−3.18	−5.91	2.990	18.28	16.21
18.180	3.741	−3.53	−6.04	2.554	18.49	16.78
22.533	3.420	−3.54	−5.71	2.049	18.32	17.02
22.868	3.180	−3.19	−5.12	1.797	17.81	16.72

to a good approximation,

$$B_{0v} = -7.00 + 0.065P_\lambda\,,$$
$$B'_{0v} = 16.40 + 0.014P_\lambda\,, \qquad (4.5)$$

where again C_v is in J mole^{-1}K^{-1} and P_λ in bars.

Although Eq. (4.1) is a good representation of the data, the measurements are sufficiently precise to reveal the fact that Eq. (4.1) is not the correct functional form for C_v. The deviations from the equation, although small, are systematic, and are related to the fact that $C_v(T_\lambda)$ is finite, whereas Eq. (4.1) diverges at T_λ. This has been discussed briefly elsewhere.[7]

In order to investigate the extent of the deviations of the data from the logarithmic functional form Eq. (4.1), one can consider the more general power law[6,19]

$$C_v = (A_v/\alpha_v)(|t|^{-\alpha_v} - 1) + B_{vt} \qquad (4.6)$$

which, with $\alpha_v < 0$, yields a finite $C_v(T_\lambda) = B_{vt} - A_v/\alpha_v$. In the limit as α_v vanishes, Eq. (4.6) yields Eq. (4.1). One would not necessarily expect Eq. (4.6) with $\alpha_v < 0$ and determined from a fit to experimental data to represent the asymptotic behavior of C_v. Asymptotically C_v is a linear function of C_p^{-1}, at least if C_p diverges; but this behavior cannot be observed in the present case at experimentally accessible values of $|t|$. Nonetheless, the data can be fitted well by Eq. (4.6), and one expects $\alpha_v < 0$ from such a fit to data sufficiently near T_λ if C_v is finite at T_λ. The results for $|t| \leq 3\times10^{-3}$ K were fitted to Eq. (4.6). Shown in Fig. 5 are the resulting values of α_v and α'_v. Surprisingly, α_v is not a monotonic function of P_λ, and for $P_\lambda \gtrsim 17$ bar we have $\alpha_v > \alpha'_v$, whereas for $P_\lambda \lesssim 17$ bar, $\alpha_v < \alpha'_v$. We shall return to this point when we discuss the heat capacity at constant pressure in terms of scaling in Sec. V C. In any event, $\alpha_v < 0$ and $\alpha'_v < 0$ at all except possibly the lowest pressure, suggesting that C_v is indeed finite at T_λ. At $P_\lambda = 1.6$ bar, α_v is so nearly equal to zero that experimentally it has not been distinguished from zero.

It would be very desirable to compare the present results with independent measurements by others. There have been measurements of C_v of liquid He^4 published by Lounasmaa and Kojo (LK)[20]; but a comparison is difficult because none of the data extend nearer T_λ than about 4×10^{-3} K, and most of the present results are for $|T_\lambda - T|$ less than that. In addition, LK do not give T_λ or $T_\lambda - T$, but instead report the absolute temperature to $\pm 10^{-3}$ K and the density to $\pm 10^{-4}$ g/cm^3. The resulting uncertainty in a derived $T_\lambda - T$ is about 2×10^{-3} K, and any comparison for $|T_\lambda - T| \lesssim 2\times10^{-2}$ K is meaningless because of this uncertainty. Nonetheless, we compare the results of LK with our Eqs. (4.1) and (4.2), and we expect, in the absence of inconsistencies between the LK measurements and the present results, that the fractional

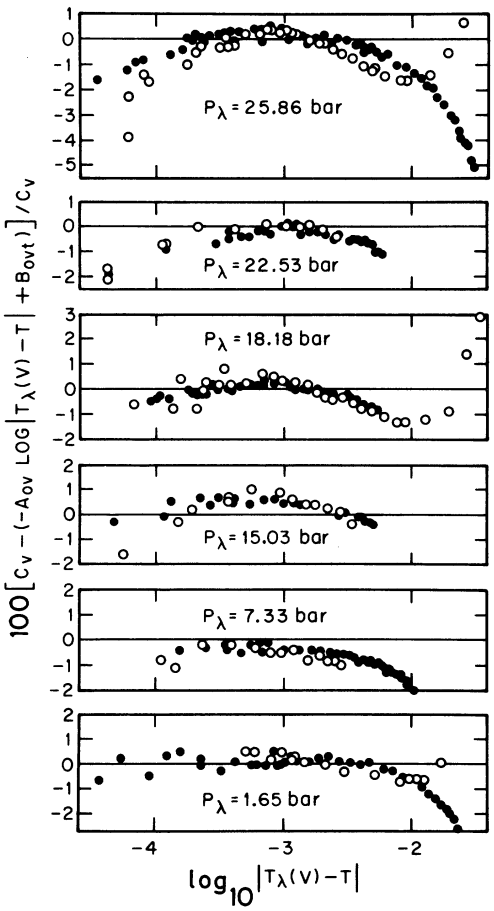

FIG. 4. Departures of individual measurements from the logarithmic functional form, Eq. (4.1), with the coefficients given by Eq. (4.2).

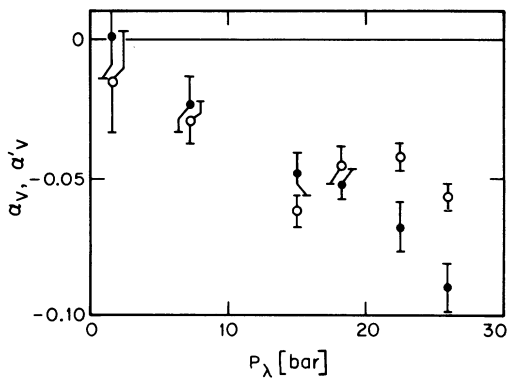

FIG. 5. Exponents α_v and α'_v obtained when the measured C_v with $|T - T_\lambda(V)| \leq 3\times10^{-3}$ K is fitted to a power law.

deviations from Eqs. (4.1) and (4.2) of data with $|T_\lambda - T| \gtrsim 2\times10^{-2}$ K should extrapolate to zero at T_λ. These deviations are shown in Fig. 6. It is apparent that the LK data can be described within a few percent by

$$C_v = (-A_{0v}\ln|t| + B_{0vt})(1+at)\,, \tag{4.7}$$

with $a = 1.7\,\mathrm{K}^{-1}$ and A_{0v} and B_{0vt} given by Eq. (4.2). An extrapolation to small $|t|$ of the deviations from Eqs. (4.1) and (4.2) does not differ significantly from zero. We thus conclude that there are no inconsistencies between the LK and the present results.

Recently, results for C_v have been reported by McCoy and Graf.[20a] These data do not agree very well with ours. They have been discussed to some extent elsewhere,[7] and the reason for the discrepancy is not known.

B. Pressure Coefficient $(\partial P/\partial T)_v$

The pressure coefficient was measured along the same six isochores and for the same values of $T_\lambda - T$ that were used for the C_v measurements, by measuring the sample pressure change which accompanied the temperature change used to determine C_v. These results are listed in Table II together with those for C_v. As with C_v, we expect $(\partial P/\partial T)_v$ to approach a finite limit, in this case less than or equal to the slope $(\partial P/\partial T)_\lambda$ of the λ line, as T_λ is approached. It already was demonstrated by Kierstead[21] that in spite of this expectation $(\partial P/\partial T)_v$ is well approximated over a wide experimentally accessible range of $T_\lambda - T$ by a linear function of $\ln|T_\lambda - T|$. This is similar to our observation for C_v.

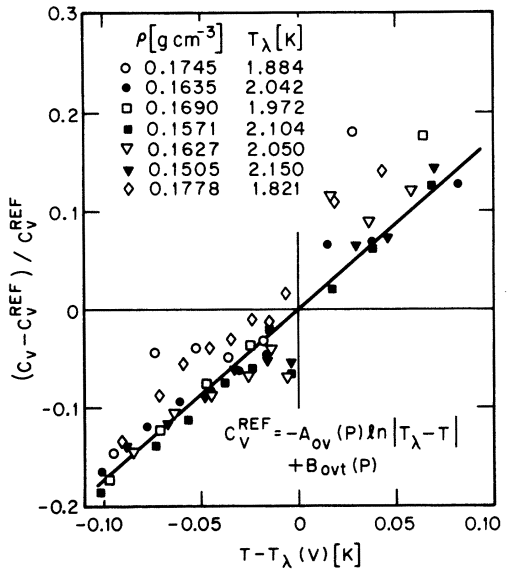

FIG. 6. Relative deviations of the results by Lounasmaa and Kojo (Ref. 20) from Eqs. (4.1) and (4.2). The deviations tend to extrapolate to zero near T_λ where Eqs. (4.1) and (4.2) apply, implying consistency with the present results.

Rather than analyzing $(\partial P/\partial T)_v$ independently as a function of $T_\lambda - T$ in a manner similar to the analysis given above for C_v, we shall consider $(\partial P/\partial T)_v$ as a function of C_v. From the total differential

$$dS = (\partial S/\partial V)_T dV + (\partial S/\partial T)_v\, dT \tag{4.8}$$

we obtain[18,22-24] with the aid of a Maxwell relation and after some rearrangement one of the so-called Pippard–Buckingham–Fairbank (PBF) relations

$$C_v/T = (\partial S/\partial T)_t - (\partial V/\partial T)_t(\partial P/\partial T)_v\,. \tag{4.9}$$

Equation (4.9) is valid along any experimental path, and in general the derivatives at constant t will be functions of t. Along isochores, however, $(\partial V/\partial T)_t$ is constant and equal to $(\partial V/\partial T)_\lambda$. The derivative $(\partial S/\partial T)_t$ must approach a finite value $(\partial S/\partial T)_\lambda$ as t vanishes, except in principle possibly at isolated singular points on the λ line, in order for the entropy to be finite along the λ line. Thus, for sufficiently small values of t, $(\partial S/\partial T)_t$ may be regarded as constant and equal to $(\partial S/\partial T)_\lambda$. Then C_v/T is a linear function of $(\partial P/\partial T)_v$. Furthermore, we emphasize that C_v/T is the *same* linear function of $(\partial P/\partial T)_v$ on the two sides of the transition, since the parameters $(\partial S/\partial T)_\lambda$ and $(\partial V/\partial T)_\lambda$ are properties of the λ line only and do not depend upon whether T_λ is approached from above or below. For this reason, a comparison of C_v with $(\partial P/\partial T)_v$ provides a valuable test of the thermodynamic consistency of measurements in the two phases. In Fig. 7 we show $(\partial P/\partial T)_v$ as a function of C_v/T for the six isochores. The measurements for He I are given as open circles, and those for He II as solid circles. It is apparent that all data on a given isochore can be represented within the scatter by the same straight line for He I and He II, provided $|T - T_\lambda| \lesssim 5\times10^{-3}$ K. We regard this as an important confirmation of the thermodynamic consistency of all the measurements, and particularly of the measurements above and below the transition. In order to demonstrate in more detail the thermodynamic consistency of the data, we have chosen the isochore $V = 22.60$ cm^3/mole, and obtained

$$(\partial S/\partial T)_t = C_v/T + (\partial V/\partial T)_\lambda(\partial P/\partial T)_v \tag{4.10}$$

from each pair of data and the least-squares value of $(\partial V/\partial T)_\lambda$. This derivative is shown as a function of $\log_{10}|T_\lambda - T|$ in Fig. 8. Again it is apparent that for small $T_\lambda - T$ the same value is obtained in He I and He II for $(\partial S/\partial T)_\lambda$.

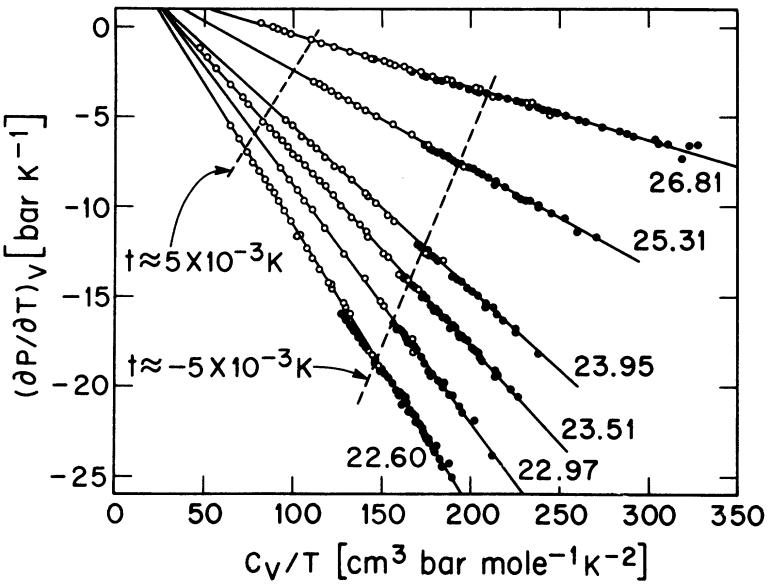

FIG. 7. Pressure coefficient $(\partial P/\partial T)_v$ as a function of C_v/T for the six isochores. Open circles: He I; closed circles: He II. The numbers near the straight lines through the data are the molar volumes. The dashed lines indicate where $T-T_\lambda$ has reached 5×10^{-3} K (He I) and -5×10^{-3} K (He II). In order to be thermodynamically consistent, the data for both phases on a given isochore must approach the same straight line for small $|T-T_\lambda|$. See Eq. (4.9).

C. Entropy, and Its Temperature Derivative at Constant $T-T_\lambda$

For many thermodynamic manipulations it is useful to know certain derivatives at constant $t=T-T_\lambda$. These derivatives may be regarded to be constant when t is sufficiently small; but it is difficult to estimate without a detailed calculation the maximum value of t at which the temperature dependence of the derivatives at constant t contributes negligibly to a given calculation. It has been shown,[25] for example, that the dependence upon t of $(\partial V/\partial P)_t$ at saturated vapor pressure is noticeable in a comparison of sound velocity[24] and C_p (Ref. 1) measurements when $t\gtrsim10^{-4}$K. On the other hand, our $(\partial P/\partial T)_v$ and C_v measurements in Fig. 7 do not reveal the t dependence of $(\partial S/\partial T)_t$ until $t\gtrsim5\times10^{-3}$ K. Thus, in general it is desirable in thermodynamic calculations to take the temperature dependence of the derivatives at constant t into consideration, if only to determine whether or not they are appreciable. We already have shown elsewhere[25] that this temperature dependence can be calculated from the heat capacity and its derivative parallel to the λ line. For the sound velocity,[24] this calculation yielded[25] accurately the correction to the asymptotic linearity of the velocity in C_p^{-1}. With the present results we have yet another opportunity to test the reliability of this type of calculation; for a combination of C_v and $(\partial P/\partial T)_v$ according to Eq. (4.10) yields directly an experimental value of $(\partial S/\partial T)_t$. The temperature dependence of this derivative can be compared with that calculated from C_v and properties of the λ line alone. For this purpose, we write the heat capacity along the experimental path in question as

$$C=-A\ln|t|+B+Dt\ln|t|+Et+Ft^2\,. \qquad (4.11)$$

In the present case, this path is of course an isochore, and $C=C_v$, $A=A_{0v}$, etc. One obtains for the entropy

$$S=S_\lambda+T_\lambda^{-1}[-At\ln|t|+(A+B)t+\tfrac{1}{2}(D+A/T_\lambda)t^2\ln|t| +\tfrac{1}{4}(2E-2B/T_\lambda-D-A/T_\lambda)t^2]\,,\quad t\equiv T-T_\lambda \qquad (4.12)$$

where terms of higher order are omitted. Differentiating at constant t,

$$\left(\frac{\partial S}{\partial T}\right)_t=\left(\frac{\partial S}{\partial T}\right)_\lambda+\left(\frac{A}{T_\lambda^2}-\frac{(\partial A/\partial T)_\lambda}{T_\lambda}\right)t\ln|t| +\left(\frac{(\partial A/\partial T)_\lambda}{T_\lambda}+\frac{(\partial B/\partial T)_\lambda}{T_\lambda}-\frac{A}{T_\lambda^2}-\frac{B}{T_\lambda^2}\right)t \qquad (4.13)$$

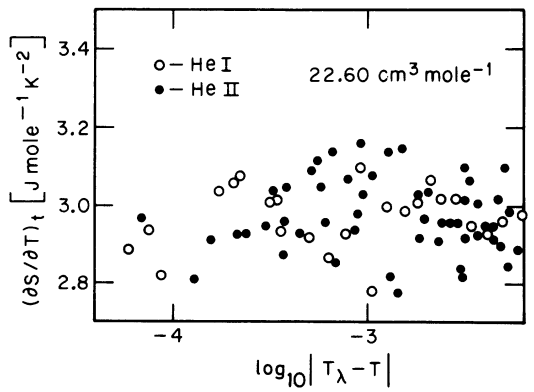

FIG. 8. Values of $(\partial S/\partial T)_t$ deduced from the measured C_v and $(\partial P/\partial T)_v$, Eq. (4.10), and the least-squares value of $(\partial V/\partial T)_\lambda$ (see text). Open circles: He I; solid circles: He II. In order to be thermodynamically consistent, the data for both phases must yield the same $(\partial S/\partial T)_t$ for small $|T_\lambda-T|$.

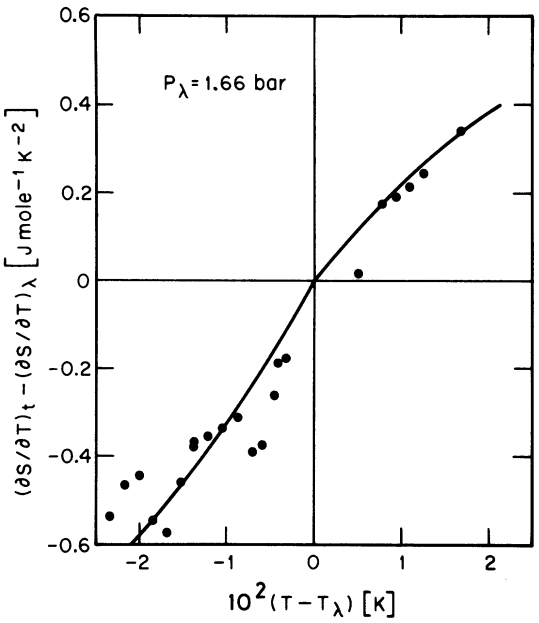

FIG. 9. Dependence of $(\partial S/\partial T)_t$ upon t. The points are from Eq. (4.10) and the measured C_v and $(\partial P/\partial T)_v$. The solid line is calculated from Eqs. (4.2) and (4.13).

which, with the definitions of A, B, and t used in Eq. (4.11) above, is consistent with Eq. (16) of Ref. 25.

For most of the present isochores, measurements were not made for sufficiently large t to reveal the dependence upon t of $(\partial S/\partial T)_t$. However, for 26.81 cm^3/mole, measurements extend to sufficiently large $|t|$ for both phases to reveal this dependence, and we show in Fig. 9 as individual symbols the experimental values for $(\partial S/\partial T)_t$ obtained from C_v, $(\partial P/\partial T)_v$, and Eq. (4.10). The solid line gives the result based on Eqs. (4.13) and (4.2). It is apparent that the agreement is very satisfactory. On the basis of this, and the work in Ref. 25, we feel that we can calculate reliably the temperature dependence of derivatives at constant t in cases where independent experimental verification is not possible. In particular, errors from this source in the calculation of C_p from C_v (Sec. IV F) are negligible.

TABLE IV. Experimental values of $(\partial S/\partial T)_\lambda$ and $(\partial V/\partial T)_\lambda$ as a function of the measured P_λ.

P_λ (bar)	$(\partial S/\partial T)_\lambda$ (J mole^{-1}K^{-2})	$(\partial V/\partial T)_\lambda$ (cm^{3}mole^{-1}K^{-1})
1.646	8.61	34.01
7.328	5.51	18.45
15.03	3.79	11.03
18.18	3.38	9.27
22.53	3.17	7.46
25.87	2.91	6.30

D. Entropy and Volume Derivatives along the λ Line

It is apparent from the discussion of Sec. IV B and Eqs. (4.9) and (4.13) that simultaneous measurements of $(\partial P/\partial T)_v$ and C_v near T_λ will yield information about the derivatives $(\partial V/\partial T)_\lambda$ and $(\partial S/\partial T)_\lambda$. These derivatives are extremely useful

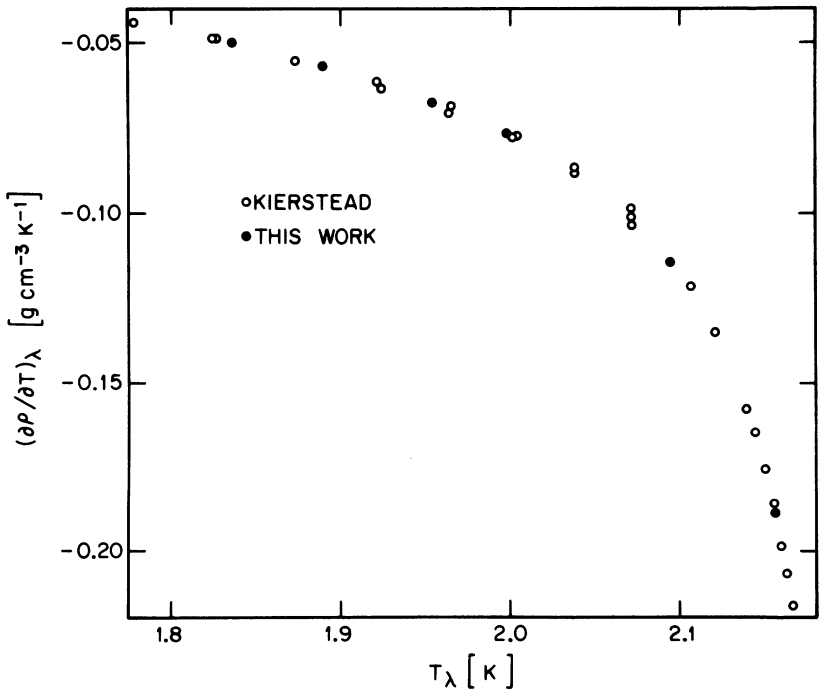

FIG. 10. Comparison of $(\partial \rho/\partial T)_\lambda$ derived from the measured C_v and $(\partial P/\partial T)_v$ with more direct measurements from Ref. 17.

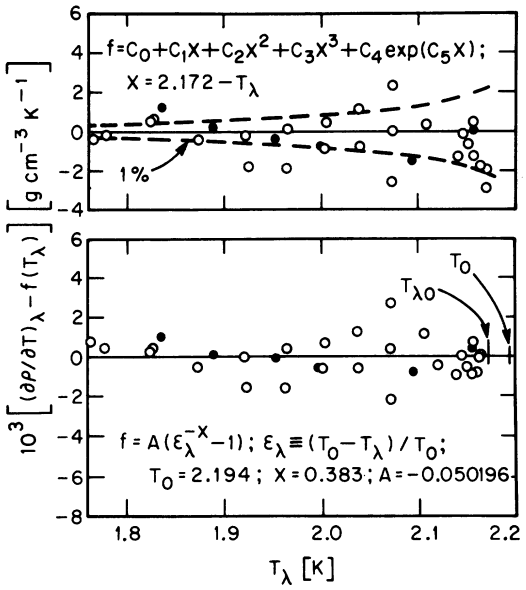

FIG. 11. Deviations of $(\partial\rho/\partial T)_\lambda$ from smooth functions $f(T_\lambda)$. Top: $f(T_\lambda)$ from Ref. 17. Bottom: $f(T_\lambda)$ given by Eq. (4.19). Open symbols are data from Ref. 17. Solid symbols are from this work.

in many thermodynamic calculations near T_λ, and they will be needed later (see Sec. IV F) in the determination of C_p from C_v. We made use of the fact that along isochores $(\partial V/\partial T)_t \equiv (\partial V/\partial T)_\lambda$, and fitted the measured C_v and $(\partial P/\partial T)_v$ to Eqs. (4.9) and (4.13) by a least-squares method. This yielded the values[7] listed in Table IV for the derivatives along the λ line. We estimate that errors in $(\partial V/\partial T)_\lambda$ are no greater than 1%, and those in $(\partial S/\partial T)_\lambda$ do not exceed 0.1 J mole^{-1}K^{-2}.

The new results for $(\partial V/\partial T)_\lambda$ can be compared with direct measurements by Kierstead,[17] who determined $(\partial\rho/\partial T)_\lambda$, where ρ is the density. We have calculated $(\partial\rho/\partial T)_\lambda$ from our $(\partial V/\partial T)_\lambda$ using the relation $(\partial\rho/\partial T)_\lambda = -(4.002/V_\lambda^2)(\partial V/\partial T)_\lambda$ and Kierstead's V_λ (see Table I) at our measured P_λ. The results are shown in Fig. 10 as solid circles. Also shown as open circles are Kierstead's measured values. Clearly, the agreement is quite good. In order to obtain greater resolution, the deviations of the data from Kierstead's equation for $(\partial\rho/\partial T)_\lambda$ are shown in the top half of Fig. 11. Although our data appear to differ from the equation systematically, the differences generally are within 1% of $(\partial\rho/\partial T)_\lambda$. This good agreement implies a high degree of thermodynamic consistency between the current results and those of Ref. 17. It strengthens our confidence in the reliability of the values for $(\partial S/\partial T)_\lambda$, which cannot be compared with equally or more precise independent measurements.

In Fig. 12 $(\partial S/\partial T)_\lambda$ is presented graphically as a function of V_λ. One finds that $(\partial S/\partial T)_\lambda$ as a function of V_λ exhibits far less curvature than it does as a function of P_λ or T_λ. Also shown in Fig. 12 is the result at SVP deduced[25] from the measured isentropic sound velocity,[24] the heat capacity at constant pressure,[1] and a thermodynamic relation similar to Eq. (4.9). All seven points can be represented, well within the expected error of 0.1 J mole^{-1}K^{-2}, by the equation

$$(\partial S/\partial T)_\lambda = A + B(V_{\lambda 0} - V_\lambda) + C(V_{\lambda 0} - V_\lambda)^2 + D(V_{\lambda 0} - V_\lambda)^3 , \tag{4.14}$$

with

$$A = 10.24 , \quad B = -3.042 , \quad C = 0.3942 , \quad D = -0.01619 . \tag{4.15}$$

Here $V_{\lambda 0} = 27.383$ cm^3 is the molar volume at saturated vapor pressure, the units of $V_{\lambda 0} - V_\lambda$ are in cm^{3}mole^{-1}, and those of $(\partial S/\partial T)_\lambda$ are in J mole^{-1}K^{-2}.

A search for an empricial relation between $(\partial S/\partial T)_\lambda$ and T_λ yielded

$$(\partial S/\partial T)_\lambda = A\epsilon_\lambda^{-x} + B , \quad \epsilon_\lambda \equiv (T_0 - T_\lambda)/T_0 \tag{4.16}$$

which, with

$$x = 1.380 , \quad T_0 = 2.260 , \quad A = 0.0938 , \quad B = 1.97 , \tag{4.17}$$

represents the data within the estimated errors. Equation (4.16) is readily integrated, and in conjunction with the calorimetric entropy at SVP[26,27] $S_{\lambda 0} = 6.24$ J mole^{-1}K^{-1}, yields the data in Table V for the entropy and its derivatives.

Possible errors in S_λ and $(\partial S/\partial T)_\lambda$ are about 1%, and $(\partial^2 S/\partial T^2)_\lambda$ may be in error by as much as 10%.

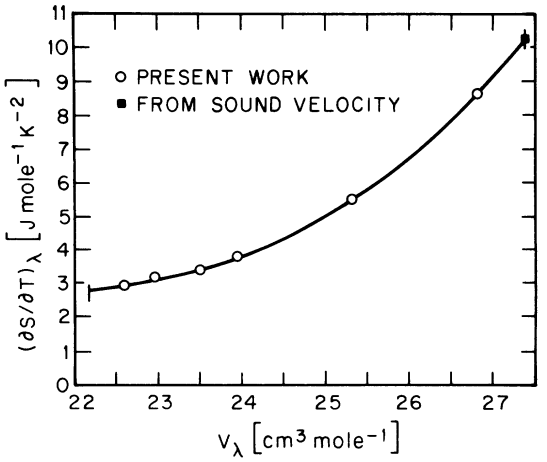

FIG. 12. Derivative $(\partial S/\partial T)_\lambda$ as a function of V_λ. The solid square is obtained in Ref. 25 from the measurements of Ref. 24.

TABLE V. Smoothed values of the entropy and its first two temperature derivatives at T_λ.

T_λ (K)	S_λ (J mole^{-1}K^{-1})	$(\partial S/\partial T)_\lambda$ (J mole^{-1}K^{-2})	$(\partial^2 S/\partial T^2)_\lambda$ (J mole^{-1}K^{-3})
2.172	6.24	10.24	129
2.17	6.22	9.99	123
2.16	6.12	8.90	96
2.14	5.96	7.36	62
2.12	5.83	6.33	43
2.10	5.71	5.00	31
2.05	5.46	4.46	16.4
2.00	5.25	3.83	9.8
1.95	5.07	3.42	6.5
1.90	4.91	3.16	4.5
1.85	4.76	2.96	3.3
1.80	4.61	2.82	2.5
1.76	4.50	2.73	2.1

In Fig. 13 the entropy S_λ computed from Eq. (4.16) is compared with calorimetric entropy data.[27,28] The agreement is quite good, and within combined possible errors.

It has been notoriously difficult in the past to find suitable empirical functions for the representation of derivatives along the λ line. Particularly near vapor pressure, derivatives with respect to T_λ tend to vary rapidly although they remain finite and nonzero.[17,29] In order to represent this behavior, Kierstead[17] used an empirical function with six parameters to represent $(\partial\rho/\partial T)_\lambda$. The success of Eq. (4.16) for fitting $(\partial S/\partial T)_\lambda$ with a much smaller number of parameters suggested that similar simple functional forms might also be useful to represent other derivatives along the λ line. The results by Kierstead[17] and our own values for $(\partial\rho/\partial T)_\lambda$, yielded the parameters

$$T_0 = 2.194\ \text{K}, \quad x = 0.383, \quad A = -0.05020 \tag{4.18}$$

for the function

$$(\partial\rho/\partial T)_\lambda = A(\epsilon_\lambda^{-x} - 1), \quad \epsilon_\lambda \equiv (T_0 - T_\lambda)/T_0 . \tag{4.19}$$

The standard deviation of the data from Eqs. (4.18) and (4.19) was only 1.0×10^{-3} g cm^{-3}K^{-1}, which is slightly smaller than but not appreciably different from the standard deviation obtained with Kierstead's six-parameter equation. In the bottom half of Fig. 11, the deviations from Eqs. (4.18) and (4.19) are shown, and they are seen to be reasonably random They can be compared readily with the deviations from Kierstead's six-parameter equation, which are shown in the top half of Fig. 11. It is apparent that Eqs. (4.18) and (4.19) are an equally good representation of the data.

We have not yet found an equally simple form for $(\partial P/\partial T)_\lambda$ which fits the measurements[17,29] within the scatter. However, $(\partial\rho/\partial P)_\lambda$, which may be obtained from the measured $(\partial P/\partial T)_\lambda$ and Eqs. (4.18) and (4.19), can be represented quite well by

$$(\partial\rho/\partial P)_\lambda = A\epsilon_\lambda^{-x} + B, \quad \epsilon_\lambda \equiv (T_0 - T_\lambda)/T_0 , \tag{4.20}$$

with parameters

$$A = 3.975\times10^{-4}, \quad B = 0.118\times10^{-4}, \quad T_0 = 2.206\ \text{K}, \quad x = 0.403 . \tag{4.21}$$

One can readily compute $(\partial P/\partial T)_\lambda$ from Eqs. (4.19) and (4.20), but the fit to the measurements[17] is not quite as good as that obtained with Kierstead's six-parameter equation. For $T_\lambda \gtrsim 2.05$ K, deviations of the measured $(\partial P/\partial T)_\lambda$ from Eqs. (4.19) and (4.20) appear random. At $T_\lambda \cong 1.95$ and 1.77 K the calculated value seems 0.6% low and 1.0% high, respectively.

E. Comparison with Other Results for $(\partial P/\partial T)_v$

Equations (4.1) and (4.2) enable us to calculate C_v to within about 1% on any isochore over the existence range of the liquid, provided $10^{-4} \lesssim |t| \lesssim 5\times10^{-3}$ K. In addition, if we also use Eq. (4.9), we can obtain an approximate closed form expression for $(\partial P/\partial T)_v$ which we estimate to be valid to about $\pm 2\%$ over the same range of $|t|$. Specifically, we shall write

$$(\partial P/\partial T)_v = a\ln|t| + b, \quad t \equiv T - T_\lambda(V) \tag{4.22}$$

with

$$a = A_{0v}/[T(\partial V/\partial T)_\lambda], \tag{4.23}$$

$$b = -[B_{0vt}/T - (\partial S/\partial T)_\lambda]/(\partial V/\partial T)_\lambda \tag{4.24}$$

for He I, and similarly with primed coefficients for He II. Here we have used the approximation $(\partial S/\partial T)_t \cong (\partial S/\partial T)_\lambda$, which was demonstrated in

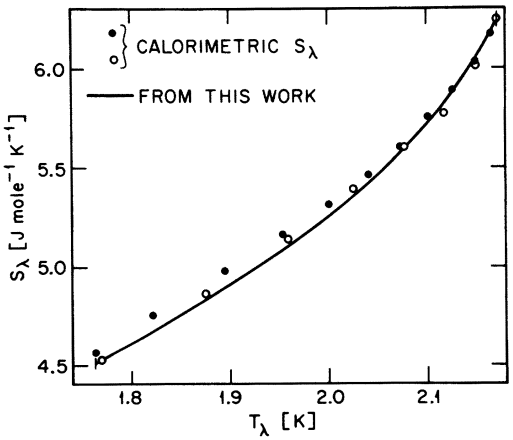

FIG. 13. Comparison of the entropy along the λ line derived from this work with calorimetric entropies at T_λ. Open circles: Ref. 28; solid circles: Ref. 27.

Sec. IV C and Fig. 7 to be valid within the requited precision over the range of t under consideration. We obtain $(\partial V/\partial T)_\lambda$ from Ref. 17 or Eq. (4.19) and $(\partial S/\partial T)_\lambda$ from Eq. (4.16).

Now it is possible to compare the present results with measurements by others of $(\partial P/\partial T)_v$ near T_λ along any isochore. Sufficiently near T_λ such measurements were made by Kierstead,[21] and by Lounasmaa.[30] The values of a, b, a', and b' corresponding [in units which yield $(\partial P/\partial T)_v$ in bar K^{-1}] to the coefficients given by the original authors, are compared with the ones based on the present work in Table VI. At 13.2 bar the coefficients of Lounasmaa appear to differ considerably from the present ones; however, either set of coefficients fits the data in Ref. 30 within the scatter for $10^{-5} \leq |t| \leq 10^{-1}$K, except possibly for He II and $|t| \lesssim 10^{-4}$K, where deviations from Eq. (4.22) with coefficients from this work appear slightly systematic. At 30 bar, the coefficients based on Kierstead's work are in good agreement with the present work, and of course the predicted values of $(\partial P/\partial T)_v$ based on either set of coefficients is in excellent agreement with the data. We note here that Kierstead's coefficients yield $a/a' = 2.117$, and the present work, extrapolated to 30 bar, gives $a/a' = 2.083$, differing by only 0.034, or 1.6% of a/a'. This agreement in the amplitudes will be important in Sec. V, when we discuss the heat capacity at constant pressure in terms of scaling predictions.

F. Heat Capacity at Constant Pressure C_p

1. C_p along Isochores

In order to calculate C_p from C_v, we write the thermodynamic relation between these two quantities in the form

$$C_p - C_v = -T\left(\frac{\partial P}{\partial T}\right)_v^2 \left(\frac{\partial V}{\partial P}\right)_T . \tag{4.25}$$

We take $(\partial P/\partial T)_v$ from our direct measurements, and write $(\partial V/\partial P)_T$ in terms of thermodynamic parameters of the λ line and C_p. Equation (4.25) can then be solved for C_p. We prefer this approach to using the relation $C_p - C_v = T(\partial P/\partial T)_v(\partial V/\partial T)_P$, which is formally equivalent to Eq. (4.25), because

TABLE VI. Comparison of parameters for $(\partial P/\partial T)_v$ from this work with measurements by others.

Source	P_λ (bars)	He I a	He I b	He II a'	He II b'
Ref. 30	13.21	1.50	3.55	1.01	−6.08
This work	13.21	1.653	4.662	1.267	−4.308
Ref. 21	29.95	3.301	9.12	1.559	−14.40
This work	29.95	3.241	9.035	1.556	−13.62

$(\partial V/\partial P)_T$, although divergent at T_λ, varies little over the experimental temperature range and is nearly equal to $(\partial V/\partial P)_\lambda$, which is known with high precision. On the other hand, $(\partial V/\partial T)_P$ changes considerably over the range of $T - T_\lambda$ of interest, and small systematic errors in $(\partial V/\partial T)_P$ could have a larger effect upon the t dependence of C_p than similar errors in $(\partial V/\partial P)_T$. We use the relation[25]

$$T\left(\frac{\partial V}{\partial P}\right)_T = -\left(\frac{\partial T}{\partial P}\right)_t^2 C_p + T\left(\frac{\partial S}{\partial P}\right)_t \left(\frac{\partial T}{\partial P}\right)_t + T\left(\frac{\partial V}{\partial P}\right)_t , \tag{4.26}$$

where $t \equiv T_\lambda(V) - T$. This and Eq. (4.25) yield

$$C_p = \left\{C_v - T\left(\frac{\partial P}{\partial T}\right)_v^2 \left[\left(\frac{\partial S}{\partial T}\right)_t \left(\frac{\partial T}{\partial P}\right)_t^2 + \left(\frac{\partial V}{\partial T}\right)_t \left(\frac{\partial T}{\partial P}\right)_t\right]\right\} \times \left[1 - \left(\frac{\partial P}{\partial T}\right)_v^2 \left(\frac{\partial T}{\partial P}\right)_t^2\right]^{-1} . \tag{4.27}$$

Aside from C_v, the major contribution to the dependence upon t in Eq. (4.27) for C_p comes from $(\partial P/\partial T)_v$. It is therefore particularly important that the best and most consistent available values be used for this quantity. It was mentioned in Sec. III B that the random errors in $(\partial P/\partial T)_v$ tend to be somewhat larger than those in C_v. In addition, values of $(\partial P/\partial T)_v$ were not obtained for every value of C_v (see Table II). For these reasons, the least-squares parameters for $(\partial S/\partial T)_\lambda$ and $(\partial V/\partial T)_\lambda$ obtained for a given isochore (see Table IV) were used along that isochore to calculate $(\partial P/\partial T)_v$ from the measure C_v [Eq. (4.9) and Eq. (4.13)]. When in the course of this analysis the value of $(\partial S/\partial T)_t$ in Eq. (4.9) was approximated by $(\partial S/\partial T)_\lambda$ instead of using Eq. (4.13), the resulting values of C_p differed from the correct value by no more than 0.6% for $|t| \lesssim 10^{-2}$K. Therefore $(\partial P/\partial T)_v$ could be expressed sufficiently accurately by Eqs. (4.9) and (4.13), and this smoothing procedure eliminated unnecessary scatter due to the lesser precision of $(\partial P/\partial T)_v$ from the final values of C_p. Possible systematic errors in C_p will be investigated later (see Sec. V B) by varying the parameters of the λ line within permitted ranges. It now remains to evaluate those contributions to Eq. (4.27) which depend only very mildly upon t.

An expression for $(\partial S/\partial T)_t$ in terms of measured quantities already has been discussed in Sec. IV C, and is given by Eq. (4.13). Along isochores $(\partial V/\partial T)_t \equiv (\partial V/\partial T)_\lambda$, and $(\partial V/\partial T)_\lambda$ is available either from the present measurements [Sec. IV D and Eq. (4.19)] or from independent determinations.[17] It remains only to obtain $(\partial T/\partial P)_t$ before C_p can be evaluated. For this purpose, we first solve Eq. (4.9) for $(\partial P/\partial T)_v$, use Eq. (4.13) for $(\partial S/\partial T)_t$,

and integrate along an isochore to obtain P as a function of t. One gets, to order $t\ln|t|$ and t,

$$P = P_\lambda + (\partial S/\partial V)_\lambda t - (\partial T/\partial V)_\lambda (S - S_\lambda) , \qquad (4.28)$$

where Eq. (4.12) gives the necessary $S - S_\lambda$. Differentiation at constant t yields

$$\left(\frac{\partial P}{\partial T}\right)_t = \left(\frac{\partial P}{\partial T}\right)_\lambda + \left(\frac{\partial^2 S}{\partial V \partial T}\right)_\lambda t - \left(\frac{\partial^2 T}{\partial V \partial T}\right)_\lambda (S - S_\lambda) - \left(\frac{\partial T}{\partial V}\right)_\lambda \left[\left(\frac{\partial S}{\partial T}\right)_t - \left(\frac{\partial S}{\partial T}\right)_\lambda\right] , \qquad (4.29)$$

which may be evaluated with the aid of Eqs. (4.12) and (4.13). Now all contributions to Eq. (4.27) are expressed to order t and $t\ln|t|$ in terms of measured quantities, and C_p can be evaluated.

As pointed out in Sec. IV C, we have considerable faith in our ability to calculate the dependence upon $T - T_\lambda$ of such quantities as $(\partial T/\partial P)_t$ [i.e., Eq. (4.29)], because of the success of such calculations to order t and $t\ln|t|$ in predicting[25] the isentropic sound velocity from C_p, and because of the comparison with direct measurements of $(\partial S/\partial T)_t$ in Fig. 9 of this paper. Nonetheless, it is difficult to estimate the size of possible systematic errors in a particular case like, for example, Eqs. (4.27) and (4.29). For this reason, C_p was calculated also in the approximation that $(\partial T/\partial P)_t$ and $(\partial S/\partial T)_t$ in Eq. (4.27) are independent of t and equal to their values at T_λ. This approximation to C_p never differed from the exact expression by more than 0.5% for $|t| \leq 3\times10^{-2}$ K. Since the effect upon C_p of the dependence upon t of $(\partial T/\partial P)_t$ and $(\partial S/\partial T)_t$ is so small, it is clear that there is no appreciable contribution to the errors of C_p from this source.

2. C_p along Isobars

Although we have obtained in the previous section values of C_p, these values are still along the experimental path, i.e., essentially along an isochore. Along isochores, the pressure varies in accordance with Eq. (4.28). The transition temperature $T_\lambda(P)$, when regarded as a function of pressure, may be considered as a variable along this path, and is different from $T_\lambda(V)$, i.e., from the transition temperature at the volume of the isochore. When we wish to express C_p as a function of $T - T_\lambda$, we therefore shall have to make a choice of whether we wish to consider C_p as a function of $T - T_\lambda(V)$, which we have at present, or as a function of $T - T_\lambda(P)$, which we can calculate from available thermodynamic information. Since it appears more consistent to regard an isobar as a "natural" path for the heat capacity at constant pressure, we shall compute C_p along isobars from our known C_p along isochores. For this purpose we define

$$\theta \equiv T - T_\lambda(P) , \quad t \equiv T - T_\lambda(V) \qquad (4.30)$$

for every point on our isochore. The difference between θ and t is illustrated schematically in Fig. 14. We shall carry out the computation of C_p along isobars in two steps. First, we compute θ from t. This is easily done, for we already know the pressure along isochores from Eq. (4.28). Now

$$\theta = t + (P - P_\lambda)(\partial T/\partial P)_\lambda . \qquad (4.31)$$

Equation (4.31) is valid as long as the λ line may be regarded as locally linear. Since $|P - P_\lambda|$ never exceeds a few tenths of a bar, this is true for all practical purposes. We now know the desired "distance" along the temperature axis from the λ line. However, we still do not in principle have C_p along isobars, for all values of C_p still have to be adjusted to some constant pressure, say P_λ for our isochore, along a path of constant θ. This second correction is numerically small, and easy to apply. It is illustrated in Fig. 14 by the dashed arrow from the experimental point 1 to the desired point 2. We first neglect the correction and obtain an approximate functional form for $C_p(\theta, P)$. Then we use this function to calculate $(\partial C_p/\partial P)_\theta$, and obtain

$$C_p(\theta, P_\lambda) = C_p(\theta, P) + (P_\lambda - P)(\partial C_p/\partial P)_\theta , \qquad (4.32)$$

where again $P - P_\lambda$ is given by Eq. (4.28). The resulting values of $C_p(\theta, P_\lambda)$ and θ are listed in Table II.

The difference between $C_p(\theta, P)$ and $C_p(\theta, P_\lambda)$, given by Eq. (4.32), always is very small (less

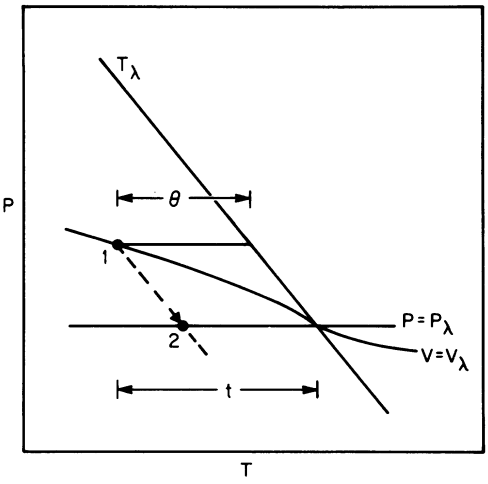

FIG. 14. Schematic representation of an isochore and an isobar near the λ line which demonstrates the conversion of t to θ and $C_p(\theta, P)$ to $C_p(\theta, P_\lambda)$ as discussed in the text.

than 0.5% even well away from T_λ) and therefore can be calculated sufficiently accurately to cause negligible errors. However, the difference between t and θ, given by Eq. (4.31), becomes large at the higher pressures, and t/θ for some of our data is as big as 1.6. More detailed values of t/θ can be obtained readily from Table II. Although we estimate that errors in this ratio are never larger than about ± 0.01, it is not immediately obvious whether or not appreciable errors may arise from this source in derived parameters. Therefore we shall return to this point later in the paper when the scaling parameters which describe C_p are discussed (see Sec. V B).

G. Heat Capacity at Constant Chemical Potential C_μ

Since it is not entirely clear which temperature derivative of the entropy should be examined for its asymptotic behavior and compared with scaling theory,[3,4] we will consider in this section the heat capacity at constant chemical potential

$$C_\mu \equiv T(\partial S/\partial T)_\mu \ . \tag{4.33}$$

It has been observed[31] that, although C_μ may in some sense be more fundamental than C_p, for the λ transition "all singularities will be unchanged, however, if the experiments are done at constant pressure." We will examine explicitly the relation between C_p and C_μ, and assure ourselves that the difference between them may indeed be ignored for our purposes. We have at constant μ from the total differential of $S(P, T)$ and with the aid of the Maxwell relation $(\partial S/\partial P)_T = -(\partial V/\partial T)_P$,

$$C_\mu = C_p - T(\partial V/\partial T)_P(\partial P/\partial T)_\mu \ . \tag{4.34}$$

Now, since $(\partial P/\partial T)_\mu = -(\partial \mu/\partial T)_P/(\partial \mu/\partial P)_T = S/V$, we obtain

$$C_\mu = C_p - (TS/V)(\partial V/\partial T)_P \ . \tag{4.35}$$

We can express $(\partial V/\partial T)_P$ in terms of C_p, and have

$$T(\partial V/\partial T)_p = (\partial T/\partial P)_\theta C_p - T(\partial S/\partial P)_\theta \ . \tag{4.36}$$

Remembering that on an isobar $(\partial T/\partial P)_\theta \equiv (\partial T/\partial P)_\lambda$, we can now write Eq. (4.35) as

$$C_\mu = [1 - (S/V)(\partial T/\partial P)_\lambda]C_p + (ST/V)(\partial S/\partial P)_\theta \ . \tag{4.37}$$

Since all quantities except C_p on the right of Eq. (4.37) are finite at T_λ, it is obvious that C_μ has indeed the same asymptotic singularity as C_p. It only remains to examine the size of possible differences in higher-order contributions, which, if they are too large, might confuse the analysis of experimental data for the asymptotic behavior. For this purpose, we first examine the term $(S/V)(\partial T/\partial P)_\lambda$. Although both the entropy and the volume on an isobar depend upon θ, this dependence is mild, and we shall examine the size of this correction at T_λ. We have $(S_\lambda/V_\lambda)(\partial T/\partial P)_\lambda \cong 0.02$ at vapor pressure and 0.04 at the solidification pressure. Since this term is small compared to unity, it is clear from Eq. (4.37) that it yields no large higher-order contributions to C_p from the leading term in C_μ and the θ dependence of S/V. Next we examine the last term in Eq. (4.37). Every contribution to this term depends upon θ, but is finite at T_λ. Again we find that at $\theta \approx 10^{-3}$ K this term contributes 1 or 2% to C_μ, and it cannot yield any large higher-order terms. We therefore conclude that the asymptotic behavior of C_p is the same as that of C_μ, and that higher-order terms, although in principle different, are of the same magnitude for C_p along an isobar as they are for C_μ along an isobar.

Finally we consider the possibility that there is an appreciable difference in higher-order contributions to C_μ along different thermodynamic paths. In principle, one might regard C_μ along a path of constant chemical potential as the most fundamental quantity. One has $(\partial \mu/\partial T)_P = -S$, and thus, along an isobar,

$$\mu - \mu_\lambda = -\int_{T_\lambda}^{T} S dT' \cong -\theta S_\lambda \tag{4.38}$$

and therefore, as in the derivation of θ from t in Sec. IV F 2,

$$\theta_\mu = \theta_P + \theta_P S_\lambda (\partial T/\partial \mu)_\lambda \ . \tag{4.39}$$

Now $(\partial T/\partial \mu)_\lambda = [-S + V(\partial P/\partial T)_\lambda]^{-1}$, and

$$\theta_\mu = \theta_p\{1 - S_\lambda/[S_\lambda - V(\partial P/\partial T)_\lambda]\} \ . \tag{4.40}$$

Here $\theta_\mu = T - T_\lambda(\mu)$, and $\theta_p = T - T_\lambda(P)$. We find that $|1 - \theta_\mu/\theta_p| \lesssim 0.02$, and virtually independent of θ_p. Thus, no large higher-order terms can arise from the path dependence of C_μ.

H. Thermodynamics on Isobars

1. *Equations for C_p*

In order to facilitate thermodynamic calculations, it is convenient to have an expression for C_p along isobars in closed form. It has been shown for the results at vapor pressure[1,2] that the function

$$C_p = -A_{0\epsilon} \ln|\epsilon| + B_{0\epsilon} + D_{0\epsilon}\epsilon \ln|\epsilon| + E_{0\epsilon}\epsilon \tag{4.41}$$

or

$$C_p = -A_{0\theta} \ln|\theta| + B_{0\theta} + D_{0\theta}\theta \ln|\theta| + E_{0\theta}\theta \ , \tag{4.42}$$

with $\epsilon \equiv \theta/T_\lambda = (T - T_\lambda)/T_\lambda$, fits those measurements extremely well over a considerable range of ϵ or θ. This function was used for the present results, and so far as possible the pressure dependence of the coefficients was determined. The

equations

$$
\begin{aligned}
A'_{0\epsilon} &= 5.102 - 0.05652P_\lambda + 9.643\times10^{-4}P_\lambda^2 ,\\
B'_{0\epsilon} &= 15.57 - 0.3601P_\lambda + 4.505\times10^{-3}P_\lambda^2 ,\\
D'_{0\epsilon} &= -14.5 + 6.119P_\lambda ,\\
E'_{0\epsilon} &= 69.0 + 19.08P_\lambda ,\\
A_{0\epsilon} &= 5.357 - 0.03465P_\lambda + 8.447\times10^{-4}P_\lambda^2 ,\\
B_{0\epsilon} &= -7.75 - 0.362P_\lambda - 4.535\times10^{-4}P_\lambda^2 ,\\
D_{0\epsilon} &= 14.5 - 6.203P_\lambda ,\\
E_{0\epsilon} &= 103 - 16.55P_\lambda ,
\end{aligned}
\tag{4.43}
$$

with P_λ in bars yield C_p in J mole^{-1}K^{-1}, and in conjunction with Eq. (4.41) are a good description of all the measurements. Deviations of most of the data from these equations in percent are shown in Fig. 15 for He I and in Fig. 16 for He II. Although these equations clearly are suitable to represent C_p in thermodynamic calculations, we caution the reader that no excessive theoretical significance should be attached to the functional form of Eq. (4.41) or the values given by Eq. (4.43) for the coefficients; for Eqs. (4.41) and (4.43) are by no means unique, and many other forms could conceivably represent the data equally well. We shall discuss this matter in detail in Sec. V.

Equation (4.41) gives C_p as a function of ϵ. Although this is convenient in many respects, we shall carry out our thermodynamic calculations in terms of $\theta = T - T_\lambda = T_\lambda\epsilon$, and make extensive use of Eq. (4.42). The coefficients of Eq. (4.42) are given in terms of those for Eq. (4.41) by

$$A_{0\theta} = A_{0\epsilon} , \tag{4.44}$$

$$B_{0\theta} = B_{0\epsilon} + A_{0\epsilon}\ln(T_\lambda) , \tag{4.45}$$

$$D_{0\theta} = D_{0\epsilon}/T_\lambda , \tag{4.46}$$

$$E_{0\theta} = [E_{0\epsilon} - D_{0\epsilon}\ln(T_\lambda)]/T_\lambda \tag{4.47}$$

for He I, and by the same relations between primed coefficients for He II.

2. *Other Thermodynamic Functions*

The thermal expansion coefficient α is readily obtained from C_p by the technique already employed in Sec. IV B to derive Eq. (4.9). One has

$$\left(\frac{\partial V}{\partial T}\right)_P = -\left(\frac{\partial T}{\partial P}\right)_\lambda \left(\frac{\partial S}{\partial T}\right)_\theta + \left(\frac{\partial T}{\partial P}\right)_\lambda \frac{C_p}{T} . \tag{4.48}$$

Here we have used the fact that on isobars $(\partial T/\partial P)_\theta = (\partial T/\partial P)_\lambda$. Since Eq. (4.42) for C_p has the same form as Eq. (4.11), it is clear that Eq. (4.12) for the entropy and Eq. (4.13) for $(\partial S/\partial T)_t$ may be used along isobars as well, provided t is

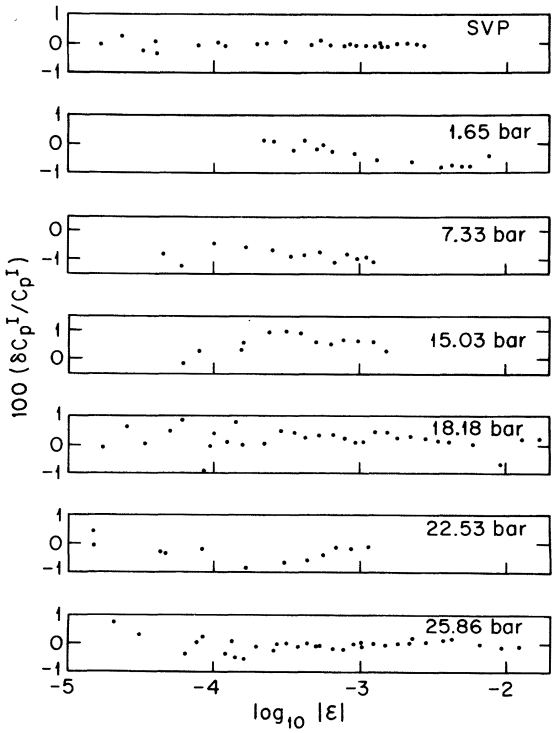

FIG. 15. Deviations in percent of C_p for He I along isobars from the reference equation, Eq. (4.41), with the least-squares adjusted coefficients given by Eq. (4.43).

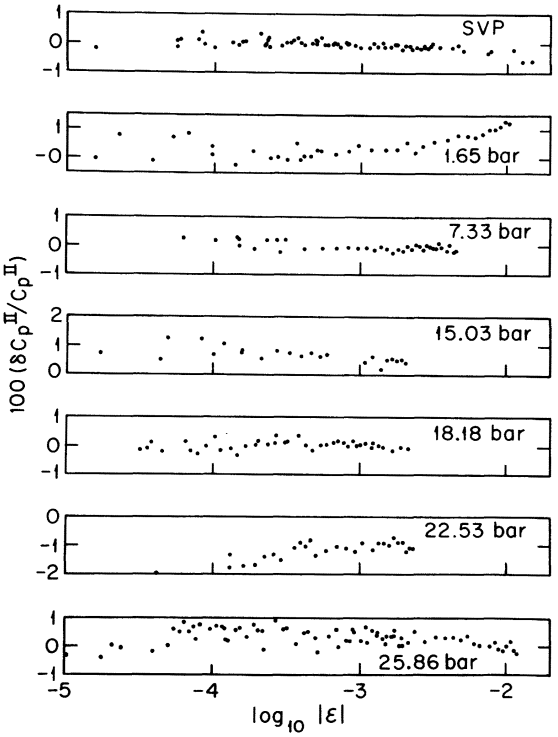

FIG. 16. Deviations in percent of C_p for He II along isobars from the reference equation, Eq. (4.41), with the least-squares adjusted coefficients given by Eq. (4.43).

TABLE VII. Thermodynamic properties of He^4 on isobars near the superfluid transition.

$\log_{10}\lvert\theta\rvert$	α (K^{-1})	κ (bar^{-1})	C_p (J $mole^{-1}K^{-1}$)	γ	$\log_{10}\lvert\theta\rvert$	α (K^{-1})	κ (bar^{-1})	C_p (J $mole^{-1}$ K^{-1})	γ
		He II, 0.05 bar					He II, 15.0 bar		
−5	−0.0836	0.0150	78.2	1.0368	−5	−0.1648	0.00842	65.7	1.307
−4	−0.0661	0.0148	66.5	1.0271	−4	−0.1356	0.00802	55.5	1.247
−3	−0.0486	0.0146	54.6	1.0178	−3	−0.1068	0.00763	45.3	1.188
−2	−0.0311	0.0144	42.3	1.0095	−2	−0.0787	0.00723	35.1	1.131
		He I, 0.05 bar					He I, 15.0 bar		
−5	−0.0535	0.0147	58.0	1.0203	−5	−0.1147	0.00774	48.1	1.203
−4	−0.0351	0.0145	45.7	1.0111	−4	−0.0819	0.00730	36.5	1.137
−3	−0.0165	0.0144	33.4	1.0034	−3	−0.0496	0.00685	25.1	1.073
−2	+0.00251	0.0142	21.2	1.0001	−2	−0.0193	0.00645	14.7	1.0192
		He II, 5.0 bar					He II, 20.0 bar		
−5	−0.1205	0.01098	73.3	1.110	−5	−0.1870	0.00811	63.2	1.441
−4	−0.0980	0.01073	62.1	1.086	−4	−0.1541	0.00762	53.2	1.356
−3	−0.0756	0.01047	51.0	1.062	−3	−0.1216	0.00714	43.3	1.273
−2	−0.0532	0.01019	39.5	1.040	−2	−0.0904	0.00665	33.7	1.195
		He I, 5.0 bar					He I, 20.0 bar		
−5	−0.0821	0.01055	54.3	1.069	−5	−0.1294	0.00726	45.7	1.293
−4	−0.0579	0.01028	42.3	1.044	−4	−0.0917	0.00700	34.2	1.197
−3	−0.0337	0.01002	30.4	1.0209	−3	−0.0546	0.00615	23.0	1.105
−2	−0.0096	0.00977	18.8	1.0028	−2	−0.0210	0.00566	13.0	1.028
		He II, 10.0 bar					He II, 25.0 bar		
−5	−0.1440	0.00924	69.1	1.199	−5	−0.2149	0.00823	61.4	1.622
−4	−0.1182	0.00892	58.4	1.159	−4	−0.1771	0.00762	51.6	1.503
−3	−0.0925	0.00860	47.8	1.119	−3	−0.1400	0.00702	41.9	1.388
−2	−0.0672	0.00826	37.0	1.0811	−2	−0.1049	0.00642	32.7	1.280
		He I, 10.0 bar					He I, 25.0 bar		
−5	−0.0999	0.00870	50.9	1.1303	−5	−0.1471	0.00714	43.8	1.410
−4	−0.0716	0.00835	39.2	1.0869	−4	−0.1029	0.00642	32.3	1.273
−3	−0.0433	0.00800	27.6	1.0455	−3	−0.0598	0.00573	21.1	1.142
−2	−0.0161	0.00767	16.6	1.0105	−2	−0.0220	0.00513	11.4	1.036

replaced by θ, and provided the coefficients given by Eqs. (4.43)–(4.47) are used. In order to obtain $\alpha \equiv V^{-1}(\partial V/\partial T)_P$, one needs to integrate Eq. (4.48) to obtain V. One has

$$V = V_\lambda + (\partial T/\partial P)_\lambda \left(S - S_\lambda - \int_0^\theta (\partial S/\partial T)_{\theta'}\, d\theta'\right) , \tag{4.49}$$

which to order θ and $\theta \ln|\theta|$ yields, with Eqs. (4.12) and (4.13),

$$V = V_\lambda - T_\lambda^{-1}(\partial T/\partial P)_\lambda A_{0\theta}\,\theta \ln|\theta| - (\partial T/\partial P)_\lambda [(\partial S/\partial T)_\lambda - T_\lambda^{-1}(A_{0\theta} + B_{0\theta})]\theta . \tag{4.50}$$

For the compressibility $\kappa \equiv -V^{-1}(\partial V/\partial P)_T$ we have[25]

$$\kappa = -\frac{1}{V}\left(\frac{\partial T}{\partial P}\right)_\lambda \left[\left(\frac{\partial V}{\partial T}\right)_\theta + \left(\frac{\partial S}{\partial T}\right)_\theta \left(\frac{\partial T}{\partial P}\right)_\lambda - \left(\frac{\partial T}{\partial P}\right)_\lambda \frac{C_p}{T}\right] . \tag{4.51}$$

Equations (4.13) and (4.50) give $(\partial S/\partial T)_\theta$ and V. It remains to obtain $(\partial V/\partial T)_\theta$. This can be done by differentiation of Eq. (4.50), and yields

$$(\partial V/\partial T)_\theta = (\partial V/\partial T)_\lambda + (\partial^2 T/\partial P \partial T)_\lambda [S - S_\lambda - (\partial S/\partial T)_\lambda \theta] + (\partial T/\partial P)_\lambda [(\partial S/\partial T)_\theta - (\partial S/\partial T)_\lambda - (\partial^2 S/\partial T^2)_\lambda \theta] . \tag{4.52}$$

Equation (4.52) can be evaluated with the aid of Eqs. (4.12), (4.13), and (4.43)–(4.47).

The ratio $\gamma \equiv C_p/C_v$ is of considerable interest, and can now be easily calculated. Since C_v is finite at T_λ and C_p may diverge, γ may diverge also at T_λ. However, γ varies only slowly in accessible ranges of θ, and at vapor pressure it does not differ much from its minimum value of unity at any accessible θ. At pressures of about 25 bar γ becomes as large as 1.6 for $\theta \cong 10^{-5}$K. One can calculate γ from the relation

$$C_p - C_v = \alpha^2 VT/\kappa , \tag{4.53}$$

which yields

$$\gamma = (1 - \alpha^2 VT/\kappa C_p)^{-1} . \tag{4.54}$$

Expressions for α, V, and κ are given above in this section.

The calculation of the isentropic sound velocity u has been discussed in detail in Ref. 25. This thermodynamic velocity is useful because a comparison with velocities measured at low frequencies provides a thermodynamic consistency test between two rather different experiments, and because comparison with measurements at higher frequencies yields the dispersion in the velocity. The value u_λ of u at T_λ can be obtained from[25]

$$u_\lambda^{-2} = V_\lambda^{-2}[(\partial T/\partial P)_\lambda(\partial S/\partial P)_\lambda - (\partial V/\partial P)_\lambda]. \quad (4.55)$$

At all T, one has

$$u^2 = \gamma V/\kappa. \quad (4.56)$$

Equations (4.55) and (4.56) may be combined to yield $u - u_\lambda$. Alternately, the more complicated Eqs. (7) or (13) in Ref. 25 may be used, but yield essentially the same result.

Table VII contains values of α, κ, C_p, and γ for $\log_{10}|\theta|$ equal to -5, -4, -3, and -2 at 5-bar intervals for SVP $\leq P \leq 25$ bar. These results are calculated from the relations given in this section, and Eqs. (4.41) and (4.43) for C_p. At constant P, linear interpolation in $\log_{10}|\theta|$ introduces negligible errors. At constant $|\theta|$, graphic interpolation in P is perhaps the best procedure. Possible errors in the calculated values of α, κ, C_p, and $\gamma - 1$ are expected not to exceed 2%.

Table VIII contains values of u_λ and $u - u_\lambda$. Errors in both quantities probably do not exceed 2 or 3%.

TABLE VIII. Isentropic velocity of sound on isobars near the superfluid transition. Units are bar, K, and cm sec^{-1}.

$\log_{10}\lvert\theta\rvert$ \ P_λ / u_λ	5.00	10.00	15.00	20.00	25.00
			$u - u_\lambda$ for He II		
−6.0	63.1	64.5	68.9	76.2	85.5
−5.5	67.6	69.2	74.0	81.9	91.9
−5.0	72.9	74.6	79.9	88.6	99.5
−4.5	79.1	81.1	87.0	96.5	108.7
−4.0	86.8	89.2	95.8	106.6	120.3
−3.5	97.0	99.9	107.8	120.3	136.5
−3.0	112.2	116.1	126.0	141.6	162.2
−2.5	139.0	144.8	158.8	180.6	210.6
−2.0	195.4	205.2	229.1	265.3	318.5
			$u - u_\lambda$ for He I		
−6.0	80.5	82.2	87.9	97.7	110.2
−5.5	88.6	90.7	97.4	108.6	123.1
−5.0	98.4	101.2	109.1	122.2	139.4
−4.5	110.5	114.3	124.0	139.8	160.4
−4.0	125.9	131.1	143.2	162.8	188.4
−3.5	145.8	153.1	169.0	194.1	227.4
−3.0	172.3	183.1	204.8	238.8	284.2
−2.5	208.8	225.8	257.4	306.4	372.9
−2.0	263.2	292.8	342.9	419.1	523.2

J. Comparison with Other Results for He^4

In addition to the internal consistency of our C_v and $(\partial P/\partial T)_v$ results which was discussed in Sec. IV B and demonstrated in Fig. 7, it was already shown in Secs. IV A, IV D, and IV E that the measurements reported here are thermodynamically consistent within combined errors with independent measurements of $(\partial P/\partial T)_v$ (Refs. 21 and 30), of C_v (Ref. 20), of $(\partial V/\partial T)_\lambda$ (Ref. 17), and of S_λ.[27,28] The present results for C_p join smoothly with the previously reported[1,2] data at vapor pressure which in turn agree[1] within allowed combined errors with previous measurements. In addition, there have been measurements by Kierstead[21] and by Grilly[32] of κ along isotherms, by Elwell and Meyer[33,34] of α along isobars, and recently by McCoy and Graf[20a] of C_v along isochores with which the present work might be compared. Further, very recent results on the scattering of light by liquid helium[35–37] can be compared with κ and $\gamma - 1$ in Table VII.

At the highest pressures, the compressibility measurements by Grilly[32] suggest a roughly logarithmic divergence of κ, but they do not extend sufficiently near T_λ and are not sufficiently precise to yield quantitative information about the parameters of the logarithmic functional form. In particular, the amplitudes, which are of theoretical interest (see Sec. V), cannot be determined very precisely. The data are, however, generally consistent within about 5% with the values quoted in Table VII.

The compressibility measurements by Kierstead[21] are along the isotherm which meets the λ line at 29.95 bar and 1.7683 K. This is beyond the pressure range of the current experiments. The results are shown in Fig. 17 as a function of $\log_{10}|P_\lambda - P|$. At the top of the figure the distance $|T_\lambda(P) - T| = -|P_\lambda - P|(\partial T/\partial P)_\lambda$ from T_λ along isobars is shown as well. The data are for small $P_\lambda - P$, and can reasonably be expected to reveal the asymptotic behavior. They are consistent with a logarithmic divergence. The best straight lines through the data yield an amplitude ratio $A_0/A_0' \cong 1.16 > 1$. This ratio of the amplitudes is consistent with our C_p results, but we do not consider it justified to make a more detailed comparison because our data are for $P \leq 26$ bar, and an extrapolation to 30 bar of Eqs. (4.41) and (4.43) could introduce sizable errors. We do not expect a dramatic change over this pressure range in the amplitude ratio, however.

It has been notoriously difficult to observe the singularity of the isothermal compressibility near T_λ. This is understandable on the basis of Eq. (4.51). We expect a contribution to κ proportional to C_p which with Eq. (4.41) leads to a logarithmic divergence with amplitude equal to $(T_\lambda V)^{-1}$

$\times(\partial T/\partial P)_\lambda^2 A_0$, and a constant contribution independent of C_p which is given by

$$\kappa_0 = -V^{-1}(\partial V/\partial P)_\lambda - V^{-1}(\partial T/\partial P)_\lambda(\partial S/\partial P)_\lambda . \quad (4.57)$$

The contribution to κ_0 from $(\partial V/\partial P)_\lambda$ dominates at all accessible $(T_\lambda - T)$ particularly at low P, and makes it difficult to observe the singular part. The situation becomes more favorable at the higher pressures. In Fig. 17 the contribution from κ_0 is shown near the bottom.

It was pointed out by Kierstead[21] that his $(\partial P/\partial T)_v$ along an isochore which meets the λ line at the same point as the isotherm for his κ is thermodynamically consistent with the κ measurements. The thermodynamic relation

$$\kappa = -V^{-1}(\partial V/\partial P)_t[1 - (\partial T/\partial P)_t(\partial P/\partial T)_v]^{-1} \quad (4.58)$$

and the measured $(\partial P/\partial T)_v$ agree with the κ data. Kierstead's measured $(\partial P/\partial T)_v$ and Eq. (4.58) yield $A_0/A_0' \cong 1.2$. Again this ratio of amplitudes is significantly larger than unity and consistent with the present work.

Elwell and Meyer[33,34] have made very extensive measurements of the isobaric thermal expansion coefficient α along isobars which cover the entire existence range of the transition. These results are generally consistent within a few percent with the values quoted in Table VII, and support a logarithmic divergence for α. However, they yield $A_0/A_0' \cong 0.9$, with estimated errors[33,34] at the intermediate and higher pressures sufficiently small to yield $A_0/A_0' < 1$. This is contrary to our results for C_p and to Kierstead's results for κ and $(\partial P/\partial T)_v$. We have no explanation for this apparent discrepancy.

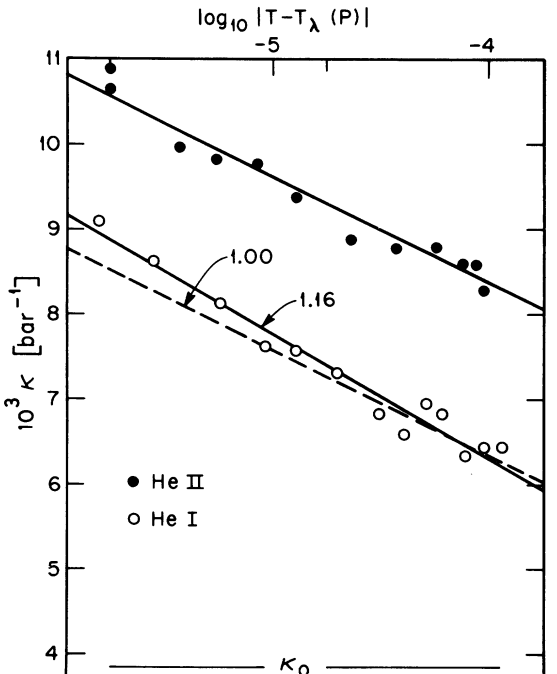

FIG. 17. Compressibility measurements from Ref. 21 along the isotherm $T = 1.7683$ K as a function of $P - P_\lambda$ on a logarithmic scale. The top of the figure is labeled by the "distance" $T - T_\lambda$ along isobars from T_λ. κ_0 is the nonsingular contribution to κ, and is given by Eq. (4.57). The numbers in the figure are the ratios of the slopes of the indicated line to that of the best line through the He II data.

The measurements by McCoy and Graf[20a] of C_v differ by as much as 12% at the higher pressures from the results of this work. They are also thermodynamically inconsistent[7] with the $(\partial P/\partial T)_v$ (Ref. 21) and the λ-line parameters[17] of Kierstead. This has been discussed in detail elsewhere.[7] We have no explanation of this difficulty.

Very recently, measurements on the scattering of light by liquid helium near T_λ have yielded thermodynamic information which can be compared with the results in Table VII. The total scattered intensity at a 90° angle to the incident light beam was measured at a pressure of about 19 bar,[35,36] and is expected to be proportional to the compressibility. Normalization at a single temperature below T_λ results in excellent agreement for all $10^{-2} \geq T_\lambda - T \gtrsim 4\times10^{-4}$ K; but in He I the normalized intensity differs from the compressibility by 2 or 3%. Although the difference for $T > T_\lambda$ is not really large, it seems slightly outside the errors of the data in Table VII since the normalization below T_λ should largely eliminate systematic errors. For $|T_\lambda - T| \lesssim 4\times10^{-4}$ K, the light scattering measurements are not expected to be simply related to κ because the inverse of the coherence length in the liquid is of the same size as the wave vector of the scattered light and hydrodynamics does not apply.

The ratio of the intensities of the Brillouin components corresponding to light scattering from thermally excited first and second sound has been measured below T_λ at pressures of 20 bar[36] and 25 bar.[37] Where hydrodynamics applies this ratio is expected to be equal to $\gamma - 1$. It agrees with the data in Table VII within the estimated uncertainties of 5–10% in the intensity ratio for $T_\lambda - T \gtrsim 10^{-4}$ K.

It can be concluded that the majority of experimental measurements of thermodynamic response functions near the λ line are consistent with each other. When fitted to a logarithmic divergence, they yield an amplitude ratio $A_0/A_0' > 1$.

V. SCALING AND UNIVERSALITY

A. Preliminary Comment

It has been shown previously[1,2] that simple-power-law interpretations, or interpretations in

terms of a logarithmic divergence with power-law correction terms, of the measured heat capacity near the superfluid transition at saturated vapor pressure are inconsistent with the Widom–Kadanoff scaling laws.[3,4] We will now examine the present results for the heat capacity at constant pressure C_p for pressures up to 26 bar from the viewpoint of scaling, and will encounter similar difficulties with simple interpretations. The most satisfactory interpretation of all the results which is in agreement with scaling is one in which the specific heat exponent α is negative, implying a finite C_p at T_λ. However, this interpretation is possible only when singular correction terms to the asymptotic behavior of C_p are allowed in the analysis. Both the leading exponent α (which is negative), and the correction term exponent are permitted by the data to be independent of the pressure P, and their best values are consistent with the results -0.02 and 0.5, respectively, which are suggested by recent calculations.[38–40] However, the ratio of the amplitude of C_p above T_λ to that below T_λ is pressure dependent. One might have expected this ratio, as well as the exponents, to be universal,[10] in the sense that changes in an "inert" variable like P would leave them unaltered. A pressure-dependent amplitude ratio also is not contained in the equation of state derived recently by Brézin *et al.*,[39] although explicit calculations have not yet been made. In addition to the difficulties with the amplitude ratio, the data and the assumption of a universal (i.e., pressure independent) $\alpha = \alpha' < 0$, also imply that C_p cannot be continuous at all pressures. For a negative leading exponent one might expect a continuous C_p because a discontinuity in some sense would correspond to a leading exponent equal to zero. Some of the results presented in this section already have been discussed briefly elsewhere.[6,8]

The predictions of scaling as they pertain to the superfluid transition have been reviewed previously in some detail.[6] We shall proceed here by analyzing the results in terms of the power law[19]

$$C_p = (A/\alpha)[|\epsilon|^{-\alpha} - 1] + B \quad \text{if } \alpha \neq 0 \tag{5.1}$$

or

$$C_p = -A_0 \ln|\epsilon| + B_0 \quad \text{if } \alpha = 0 \tag{5.2}$$

for He I, and the equivalent expression with primed coefficients for He II. Here

$$\epsilon \equiv \theta/T_\lambda = [T - T_\lambda(P)]/T_\lambda(P). \tag{5.3}$$

Equation (5.1) is equivalent to Eq. (5.2) in the limit as α vanishes; and the implication $\alpha \equiv 0$ of the form of Eq. (5.2) is indicated explicitly by the subscript on A and B.

The scaling predictions which one can attempt to test directly on the basis of the present data alone are[3,4]

$$\alpha = \alpha' \tag{5.4}$$

and

$$A = A' \text{ if } \alpha = \alpha' = 0. \tag{5.5}$$

In addition, if measurements from other sources of the superfluid density are available, we can also test the scaling law[41]

$$\zeta = 2\beta - \eta\nu', \tag{5.6}$$

which with the aid of other scaling laws[3,4] is readily written as[41]

$$\zeta = \tfrac{1}{3}(2 - \alpha'), \tag{5.7}$$

where the superfluid density $\rho_s \sim \epsilon^\zeta$, the coherence length for order-parameter fluctuations $\xi \sim \epsilon^{-\nu'}$, the order parameter $|\psi| \sim \epsilon^\beta$, and where η describes the departures of the correlation function from Ornstein–Zernike behavior. We may further consider the relation

$$B - A/\alpha = B' - A'/\alpha'. \tag{5.8}$$

In terms of the parameters of the function $C_p = A^*|\epsilon|^{-\alpha} + B^*$ which has sometimes been used by others, Eq. (5.8) is equivalent to

$$B^* = B^{*\prime}. \tag{5.9}$$

Equations (5.8) or (5.9) pertain to the parameters of C_p if, in addition to the basic homogeneity postulate of scaling, it is also assumed that the leading asymptotic singularity is the only singular term in the free energy. One might expect Eq. (5.8) or (5.9) to be valid particularly if $\alpha = \alpha' < 0$; for in that case a discontinuity in C_p, which has an exponent equal to zero, would in some sense be the leading singularity.

Although Eqs. (5.1) and (5.2) may be expected to represent the asymptotic behavior of C_p as ϵ vanishes, one must in general expect contributions to C_p which are of higher order in ϵ. We have discussed these terms to some extent when the measurements at vapor pressure were presented.[1,2] The possibility of the existence of these terms makes it extremely difficult, if not impossible, to arrive at unqualified conclusions about the asymptotic behavior of C_p, i.e., about A, A', α, and α'. Therefore we will proceed by making several sets of assumptions either about the correction terms or about the parameters of the leading term. We can then see if these assumptions and the measurements are consistent with pertinent predictions.

Before proceeding to a comparison of the measurements with the predictions, we shall first discuss in some length the size of possible errors in the scaling parameters α, α', and A_0/A_0'. The

reader who is not particularly interested in this detail may immediately proceed to Sec. V C.

B. Errors in Scaling Parameters

Of particular interest from the viewpoint of scaling are the exponents α and α' in Eq. (5.1) and the ratio A_0/A_0' of the amplitudes above and below T_λ in Eq. (5.2). These quantities are defined in terms of C_p and θ rather than in terms of the actual measured quantities C_v and t. Clearly, C_p and θ are subject to systematic errors which arise in their derivation from uncertainties in the necessary thermodynamic parameters. Before we proceed to a discussion of our experimental data in terms of the scaling laws, we must therefore consider carefully how systematic errors may propagate, and how large the resultant systematic errors in α, α', and A_0/A_0' may be. We expect that these errors will be largest at the highest pressure, because C_p/C_v and t/θ are largest there, thus requiring the largest corrections. For this reason we have chosen the measurements at 25.86 bar for a detailed investigation of the effect of changes in parameters, and have calculated α', A_0, and A_0' for the following cases:

(i) our best estimate of all parameters;
(ii) $(\partial V/\partial T)_\lambda$ was changed to 1.01 $(\partial V/\partial T)_\lambda$;
(iii) $(\partial S/\partial T)_\lambda$ was changed to 1.01 $(\partial S/\partial T)_\lambda$;
(iv) $(\partial P/\partial T)_\lambda$ was changed to 1.01 $(\partial P/\partial T)_\lambda$;
(v) $(\partial S/\partial T)_t$ was regarded as independent of t and equal to $(\partial S/\partial T)_\lambda$;
(vi) $(\partial T/\partial P)_t$ was regarded as independent of t and equal to $(\partial T/\partial P)_\lambda$;
(vii) in Eqs. (5.1) and (5.2), t/T_λ was used for ϵ instead of θ/T_λ;
(viii) T_λ was changed to $T_\lambda + 1.0\times10^{-6}$ K.

In each case, pure-power-law behavior was assumed for C_p.

We believe that these cases cover all possible sources of appreciable systematic errors in the C_v to C_p and t to θ conversion. Equations pertinent to these conversions are Eqs. (4.9), (4.13), (4.27), (4.29), and (4.31). Cases (ii)–(iv), which assume a 1% error in certain parameters, are realistic estimates of possible errors. Cases (v)–(vii) are, of course, totally unrealistic overestimates because they assume that the error in a particular correction is 100%. Case (viii) is believed to overestimate the error in T_λ by an order of magnitude. Results were obtained with assumptions (i)–(viii) at 25.86 bar, and are listed in Table IX. In each case the calculations were somewhat arbitrarily performed with all available data for which $|\theta/T_\lambda| \leq 1.58\times10^{-3}$, and included 51 points for He II and 27 points for He I. We conclude from the data in Table IX that even at our highest pressure the total systematic errors in α' (or α) and A_0/A_0' from items (ii)–(viii) above do not exceed 0.003 and 0.01, respectively.

TABLE IX. Effect of various systematic errors in the data processing on the scaling parameters at 25.86 bar.

Case	α'	A_0'	A_0	A_0/A_0'
(i)	0.002	4.148	4.802	1.158
(ii)	0.001	4.105	4.780	1.165
(iii)	0.002	4.138	4.793	1.158
(iv)	0.001	4.104	4.781	1.165
(v)	−0.001	4.178	4.798	1.148
(vi)	0.003	4.137	4.802	1.161
(vii)	0.004	4.319	5.097	1.180
(viii)	0.006	4.161	4.784	1.150

The only additional systematic errors to be considered are ones arising from systematic errors in the temperature scale. Since α, α', and A_0/A_0' are derived from measurements over an extremely narrow absolute temperature interval, they are virtually independent of the particular temperature scale which is used. Of course A_0 and A_0' by themselves will be subject to errors from this source. For this reason, we must expect a scatter of 1 or 2% in A_0 or A_0' as a function of pressure.

In addition to the systematic errors discussed above, there will be random errors for α, α', A_0, and A_0' which will depend upon the number of data points used to derive these parameters. These random errors increase rapidly as the range of ϵ over which data are included in the analysis is decreased, and will have to be indicated specifically in particular situations. As a general guide, however, random errors when data up to $\epsilon \cong 1.6\times10^{-3}$ are included, and a pure power law is assumed, are approximately ±0.005 to ±0.015 for α and α', ±0.03 J mole^{-1}K^{-1} for A_0 and A_0', and ±0.007 for A_0/A_0'.

C. Analysis without Higher-Order Singular Terms

In order to compare Eqs. (5.1) and (5.2) with the measurements, we shall assume initially, as was done at SVP, that contributions to C_p from higher-order terms in ϵ are negligible for $\epsilon \ll 1$. We expect this to be the case if these higher-order contributions arise from terms in the free energy which are regular functions of T. In this connection, we note that typical scaled equations of state that have been discussed[5] have usually assumed free energies with singularities only in the leading term. For these cases, we would expect Eqs. (5.8) and (5.9) to be valid. We have chosen, somewhat arbitrarily, a maximum value $\epsilon_{max} = 1.6\times10^{-3}$, and all data at a given pressure with $|\epsilon|$

$< \epsilon_{max}$ were fitted to Eqs. (5.1) and (5.2) to obtain α and α'. We note that, if higher-order singular terms are indeed absent in C_p, then deviations from Eqs. (5.1) and (5.2) will only be of order ϵ, and not larger than the experimental scatter for $|\epsilon| \leq \epsilon_{max}$. The results are shown in Fig. 18. The same analysis, but with $\epsilon_{max} = 3\times10^{-3}$, yielded very similar parameters, but the statistical errors were smaller. We recall that at SVP the type of analysis used here resulted in $\alpha' < \alpha = 0$,[1,2] in contradiction to Eq. (5.4). For $1.6 \leq P \leq 15$ bar, we find that within our errors, $\alpha = \alpha' = 0$. If we assume, as is permitted by our data, that $\alpha = \alpha'$ and independent of P for $P < 15$ bar, then we find an average

$$\alpha = \alpha' = 0.000 \pm 0.003 \quad \text{for } 1.6 \leq P \leq 15.0 \text{ bar}. \tag{5.10}$$

This result is consistent with scaling, i.e., with Eq. (5.4), but differs from the result at SVP. It suggests, but does not prove, that the result $\alpha' < 0$ at SVP might not be representative of the asymptotic behavior of C_p, but rather a consequence of contributions to C_p from singular higher-order terms which are larger than of order ϵ. According to this interpretation, at sufficiently small ϵ Eq. (5.10) is valid also at SVP.

At pressures greater than 15 bar, difficulties arise again when higher-order terms are assumed to be small, but this time in the high-temperature phase. We find within our errors that

$$\alpha > \alpha' = 0 \quad \text{for } 15.0 \lesssim P \leq 25.9 \text{ bar}, \tag{5.11}$$

in contradiction to Eq. (5.4). This time, α becomes as large as 0.04. Our experience with the low-temperature phase at vapor pressure, however, makes us hesitant to accept this result as representative of the asymptotic behavior. We are inclined to believe it possible that in fact $\alpha = \alpha'$ at all pressures, with higher-order contributions to C_p responsible for the apparent departures from Eq. (5.4). If we adopt this point of view, we can no longer expect Eqs. (5.8) and (5.9) to be valid. In this connection, it is interesting to note that recent measurements of the heat capacity at constant volume near the liquid-gas critical point of CO_2 (Ref. 42) are consistent with $\alpha = \alpha' > 0$, but inconsistent with Eq. (5.8). Both the present work and that of Ref. 42 lend strong support to the existence of higher-order singular terms in the free energy; but neither result is definitive about the functional form of these terms.

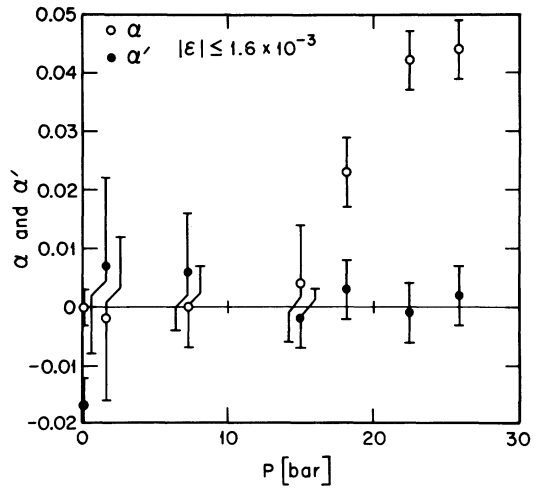

FIG. 18. Exponents α and α' of C_p which are obtained when data with $|\epsilon| \leq 1.6\times10^{-3}$ are fitted to a pure power law.

The apparent pressure dependence of α indicated in Fig. 18 seems most unusual, and should have been noticeable as an anomaly in the pressure dependence of the original data for C_v from which C_p was derived. Indeed, we have displayed in Fig. 5 values for the effective exponent α_v of C_v, and we found α_v to be nonmonotonic. Although we already have demonstrated that C_p can be calculated reliably from C_v, it is comforting to see the anomalous behavior of α reflected in the primary data.

Before we proceed to examine the results from the viewpoint that singular higher-order terms must be considered, we will first enquire whether the data and the hypothesis of no singular higher-order terms are consistent with scaling at least over the limited range $1.6 \leq P \leq 15$ bar, where the current analysis yields $\alpha = \alpha'$. Since α and α' are extremely small, and within their errors indistinguishable from zero, we shall assume that in fact $\alpha = \alpha' = 0$, and examine A_0/A_0' for $P \leq 15$ bar. In this manner we can test Eq. (5.5). We show in Fig. 19 values of A_0/A_0' which were obtained by fitting the data for $\epsilon \leq 1.6\times10^{-3}$ to Eq. (5.2). Also shown for comparison is the result at vapor pressure ($P \cong 0$), which was deduced in Ref. 1 by invoking singular higher-order terms for $T < T_\lambda$. It is clear that even over the limited pressure range $1.6 \leq P \leq 15$ bar this interpretation of the measurements is inconsistent with scaling because $A_0/A_0' \cong 1.06 \neq 1$, contrary to Eq. (5.5). This is, of course, the same observation that was made already[1,2] for the results at saturated vapor pressure.

D. Analysis with Singular Higher-Order Terms and $\alpha = \alpha' = 0$

So far, we have investigated what our data imply about scaling if it is assumed that the only singular term in the free energy is the leading asymptotic singularity. We found that this assumption and the data imply a breakdown of scaling because for $P > 15$

bar $\alpha' = 0 < \alpha$, in contradiction to Eq. (5.4), and for $P < 15$ bar, where the data yielded $\alpha = \alpha' = 0$, $A_0 > A_0'$, in contradiction to Eq. (5.5). The pressure dependence of α implied by this analysis also appears to be a breakdown of universality. We shall now investigate whether agreement with theory can be obtained if singular higher-order terms which may be large even for small $|\epsilon|$ are permitted in the analysis. Obviously it is extremely difficult in that case, if not impossible, to make quantitative statements about the asymptotic behavior of C_p without some additional assumptions either about the asymptotic functional form of C_p, or about the functional form of the higher-order terms. We shall therefore proceed by making some reasonable assumptions, and by then investigating their consequences.

Inspection of Fig. 18 reveals that, although α seems to depend upon P, α' is remarkably constant and very close to zero. In fact, if α' is assumed to be independent of P, then the data (exclusive of the vapor-pressure result) yield an average

$$\alpha' = 0.001 \pm 0.003 . \tag{5.12}$$

It is of course possible that data which include higher-order contributions yield $\alpha' = 0$ by coincidence, when in fact $\alpha' \neq 0$ corresponds to the asymptotic behavior; but we observe that $\alpha' = 0$ within error has been obtained consistently at all pressures except SVP. Thus, if the asymptotic exponent is in fact different from zero, then higher-order terms have to contribute over the experimental range of ϵ at *all* P just to the extent required

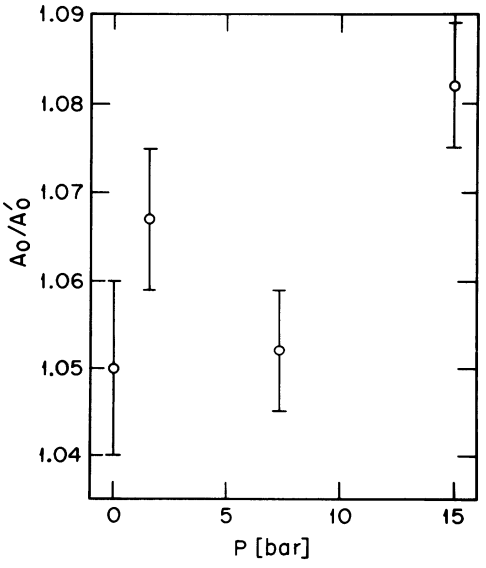

FIG. 19. Amplitude ratio A_0/A_0' of the logarithmic C_p which is obtained at low pressures when the data are fitted to a pure logarithmic divergence.

TABLE X. Parameters of Eq. (5.2) for a logarithmic C_p.

P_λ	A_0'	B_0'	A_{01}	B_{01}	A_{02}	B_{02}
SVP	5.100[a]	15.52[a]	5.355[a]	−7.77[a]		
1.65	5.036	14.82	5.374	−8.91	5.393	−9.06
7.33	4.801	12.70	5.053	−9.82	5.103	−10.29
15.03	4.501	11.35	4.846	−11.50	4.988	−12.84
18.18	4.292	11.48	4.837	−12.78	5.017	−14.52
22.53	3.991	11.94	4.819	−14.39	5.023	−16.43
25.86	4.148	10.79	4.801	−15.24	5.115	−18.26

[a]From Ref. 1.

to yield $\alpha' = 0$ from a fit to Eq. (5.1). The absence of any dependence upon P of α' in Fig. 18 therefore might suggest that $\alpha' = 0$ does indeed correspond to the asymptotic behavior. Thus, we shall explore as a second interpretation the possibility that, consistent with scaling, $\alpha = \alpha' = 0$ at all pressures. We will attempt to attribute the apparent departure in Fig. 18 of α from zero at large P to higher-order contributions to C_p. If $\alpha = \alpha' = 0$, then scaling requires $A_0 = A_0'$, according to Eq. (5.5). We have already seen in Fig. 19 that this relation is violated for $P \leq 15$ bar. We shall proceed nonetheless and examine in more detail as a function of pressure the asymmetry about T_λ which corresponds to this apparent breakdown of scaling. We do this by examining the difference

$$\Delta C_p(|\epsilon|) = C_p^{\mathrm{I}}(|\epsilon|) - C_p^{\mathrm{II}}(|\epsilon|) \tag{5.13}$$

which, with Eq. (5.2), can be written as

$$\Delta C_p(|\epsilon|) = (A_0' - A_0)\ln|\epsilon| + (B_0 - B_0') . \tag{5.14}$$

According to Eq. (5.5), the amplitude of $\ln|\epsilon|$ in Eq. (5.14) should vanish, and ΔC_p should be independent of ϵ in the limit $|\epsilon| \ll 1$. We have fitted the measurements for He II to Eq. (5.2), and list the resulting parameters in Table X. ΔC_p was evaluated by subtracting Eq. (5.2) with these He II parameters from the He I data, and is shown in Fig. 20. The curvature of the data at the higher pressures and for $\epsilon \gtrsim 5 \times 10^{-4}$ reflects the result, shown in Fig. 18, that a fit to Eq. (5.1) yields $\alpha > 0$. It is immediately apparent that the data over the entire pressure range and at all accessible ϵ do not reflect the scaling prediction $A_0 = A_0'$ because ΔC_p does not show any tendency to become independent of $|\epsilon|$ even for our smallest $|\epsilon|$. In fact, the data imply that $A_0' - A_0$ in Eq. (5.14) is nonzero, and that ΔC_p diverges as $\ln|\epsilon|$. We cannot, of course, rule out the possibility that higher-order contributions have a sufficiently complicated form to obscure completely the asymptotic behavior even at our smallest $|\epsilon|$ of about 10^{-5}.

We have seen that it is not possible to interpret the measured C_p at any pressure and over our range of ϵ in a manner consistent with scaling if $\alpha = \alpha' = 0$, because then according to the data $A_0/A_0' > 1$. Nonetheless it may be of interest to have a

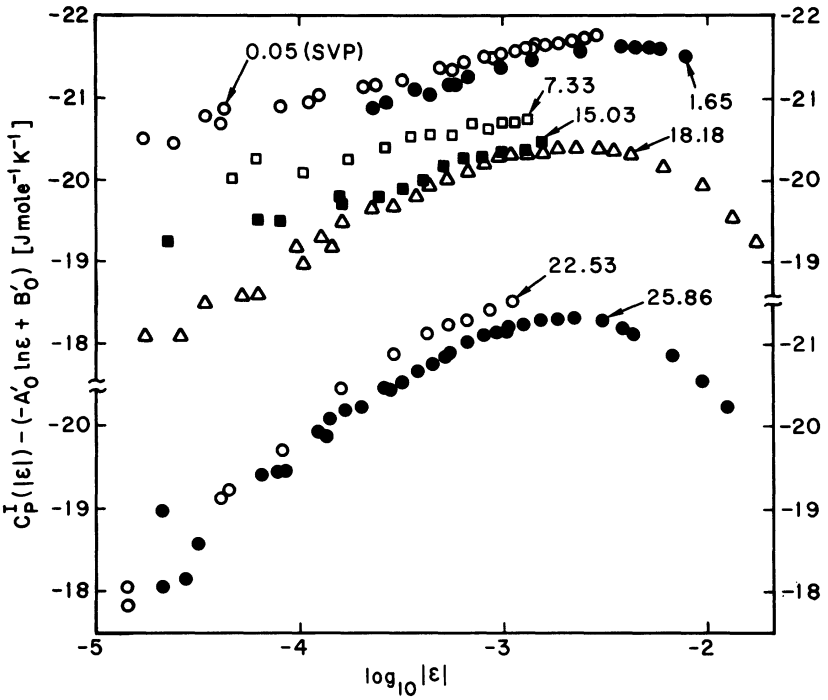

FIG. 20. Difference ΔC_p between C_p for He I and C_p for He II along isobars as a function of $\log_{10}|\epsilon|$. The numbers in the figure are the pressures in bars. Note that the data at 22.53 and 25.86 bar are displaced with respect to the other data.

reasonable estimate of the size of A_0/A_0'. As a crude approach to this problem we can simply fit the data for $\epsilon \lesssim 1.6\times10^{-3}$ to Eq. (5.2), although we know that for He I Eq. (5.1) with $\alpha > 0$ is a better fit. Inspection of Fig. 20 and the curvature of ΔC_p vs $\ln|\epsilon|$ reveal that this procedure yields a *lower limit* for A_0, and therefore for A_0/A_0'. This lower limit is given in Table X as A_{01}. The associated B_{01} is listed also. A more realistic and larger value for A_0 is obtained by making some assumption about the form of the higher-order terms that cause the curvature in Fig. 20 at the higher pressures. We have assumed, as was done at vapor pressure[1,2] for He II, that these terms can be written as $D\epsilon\ln|\epsilon| + E\epsilon$. The use of this functional form in conjunction with Eq. (5.1) yields values of α with much larger statistical errors than those shown in Fig. 18 because of the correlation between the large number of parameters in the fitting function, and in all cases the value $\alpha = 0$ is permitted by the data and this functional form. We obtain the A_{02} and B_{02} given in Table X. As a test of this estimate of A_0, we have used yet another approach which makes no assumption about the form of the higher-order terms but is possible only when data are plentiful. At 18.18 and 25.86 bar, we have fitted all data with $|\epsilon| \leq \epsilon_{max}$ to Eq. (5.2), and determined A_0 as a function of ϵ_{max}. We show the results in the top half of Fig. 21. In the bottom half of this figure the corresponding results for A_0' are shown. It is evident that A_0' within the statistical errors indicated in the figure is independent of ϵ_{max}, as it should be if Eq. (5.2) fits the data. For A_0, however, a trend with ϵ_{max} is observable which is larger than the statistical errors, indicating that Eq. (5.2) is inadequate. However, we are at the moment assuming that Eq. (5.2) is asymptotically correct, and therefore may attempt to extrapolate A_0 to $\epsilon_{max} = 0$, as shown by the solid lines. This results in $A_0 \cong 4.97$ at 18.18 bar and 5.05 at 25.86 bar. These values are lower than A_{02} by only 0.9 and 1.3%, respectively, and tend to support the validity of our previous analysis which yielded A_{02}. Best estimates with reasonable error bars for A_0/A_0' over the entire pressure range are shown in Fig. 22.

It matters little at the present which method of determining A_0/A_0' we prefer. We are forced to conclude that $A_0/A_0' > 1$ at all pressures, contrary to scaling and the assumption $\alpha = \alpha' = 0$. Further, A_0/A_0' depends appreciably upon pressure, varying from about 1.05 at vapor pressure to about 1.22 at 26 bar. The pressure dependence of A_0/A_0' seems to violate the concept of universality.

The result $A_0/A_0' > 1$ obtained from the data and the assumption $\alpha = \alpha' = 0$ which we have pursued so far has implied that higher-order terms, although they are singular and larger than of order ϵ, are sufficiently small that they can be neglected for $\epsilon \lesssim 10^{-4}$. This can be seen by inspecting Fig. 20, where ΔC_p approaches linear behavior in the vicinity of $\epsilon = 10^{-4}$ even at the higher pressures. It is of course possible that higher-order contributions are so large that they do not become negligible

compared to the leading term until ϵ is much smaller. In that case, ΔC_p in Fig. 20 might change its qualitative behavior and approach a constant at very small ϵ, and then $A_0 = A_0'$, and scaling would be valid. It is not feasible to disprove this possibility by experiment if higher-order terms are permitted to be arbitrary. However, the present data imply that if $A_0 = A_0'$, then higher-order terms are not negligible unless $\epsilon \ll 10^{-5}$, because for a larger ϵ ΔC_p in Fig. 20 depends upon ϵ. In addition, these terms would have a complicated dependence upon ϵ, and could not be represented by a simple power law over an appreciable experimentally accessible range of ϵ. Nonetheless, for completeness, let us pursue the possibility $A_0 = A_0'$ somewhat further. In this case, scaling imposes no further unsatisfied conditions upon C_p. However, if in addition to scaling it is assumed that the so-called "linear model" hypothesis[43] is valid for the parametric equation of state of Josephson[44] and Schofield,[45] then a relation exists between B_0' $- B_0$ and the exponent β for the coexistence curve. We have[46] from the linear model[43]

$$\lim_{|\epsilon|\to 0} (-\Delta C_p) = B_0' - B_0 = 2A_0'/(1-2\beta) + A_0' \ln[\beta/(1-\beta)]. \tag{5.15}$$

If we assume, consistent with the data in Fig. 20, that ΔC_p is monotonic in $|\epsilon|$ for all $|\epsilon| \lesssim 10^{-3}$, then Eq. (5.15) yields $\beta \leq 0.30$ at all pressures. In conjunction with the scaling law[3,4,41] $\eta\nu' = 2\beta - \frac{1}{3}(2 - \alpha')$ this yields $\eta < 0$, and for $\nu' \cong \frac{2}{3}$ one gets $\eta \leq -0.1$. Similarly one obtains $\gamma' \geq 1.40$ from $(2-\eta)\nu' = \gamma'$, and $\delta \geq 5.67$ from $\alpha' + \beta(1+\delta) = 2$. These exponents satisfy all the known inequalities,[47] and there is no thermodynamic stability argument against them. Nonetheless, $\eta \leq -0.1$ seems most unusual.

We have seen so far that it is virtually impossible to interpret the measurements in a manner consistent with scaling and $\alpha = \alpha' = 0$, even by invoking singular higher-order terms. Only by permitting these terms to be extremely large and of a complicated, at present apparently unreasonable, functional form can enough freedom be introduced into the interpretation to achieve consistency with $A_0 = A_0'$. Therefore we shall next pursue the possibility that higher-order terms are important in both phases, and that $\alpha = \alpha' \neq 0$. In that case scaling does not require $A = A'$.

E. Analysis with Singular Higher-Order Terms and $\alpha = \alpha' \neq 0$

As an alternate interpretation, we can consider the possibility that higher-order terms contribute appreciably in both phases at most pressures, and that in fact $\alpha = \alpha'$ at all pressures. At first, let us assume, as we did at vapor pressure,[1,2] that α and α' are equal to some value intermediate to those derived for α and α' at a given pressure in the first interpretation (Sec. V C) and shown in Fig. 18. At SVP, this approach resulted[1] in consistency with scaling, and implied a finite C_p at $\epsilon = 0$ (i.e., $\alpha = \alpha' < 0$). It is evident that we can no longer attain consistency with scaling in this manner, because $\alpha = \alpha' = 0$ would still be obtained for $1.6 \leq P \leq 15.0$ bar. Over this range, then, $A_0/A_0' > 1$, contrary to the prediction Eq. (5.5). The pressure-dependent values obtained in this manner for α and α' would violate universality.

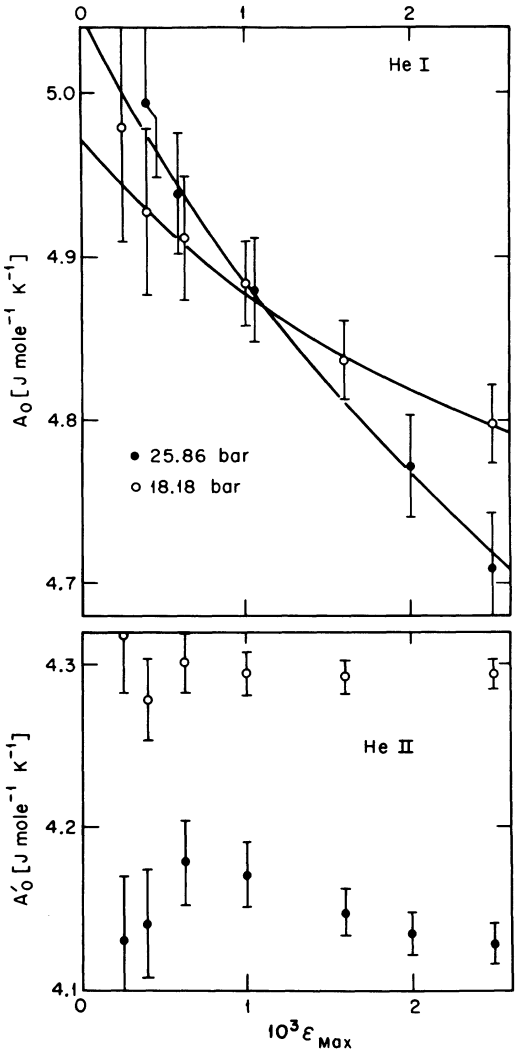

FIG. 21. Amplitudes A_0 and A_0' obtained from the measured C_p at 25.86 and 18.18 bar and a fit to the logarithmic functional form of data for which $|\epsilon| \leq \epsilon_{max}$.

It is apparent now that consistency between scaling and the data is attainable only by invoking singular higher-order contributions which result in $\alpha = \alpha' \neq 0$ at all pressures. In particular, we have chosen to write the specific heat above T_λ in the

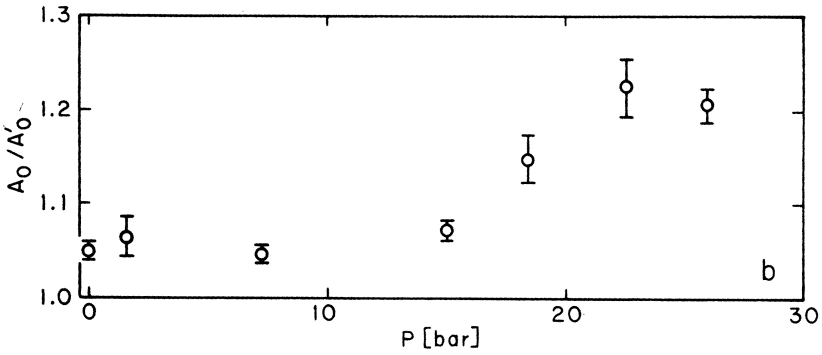

FIG. 22. Amplitude ratio A_0/A_0' of a logarithmically divergent C_p over the entire pressure range.

form

$$C_p = (A/\alpha)(|\epsilon|^{-\alpha} - 1)(1 + D|\epsilon|^{x}) + B, \qquad (5.16a)$$

with $x > 0$, and similarly with primed coefficients below T_λ. One could choose other slightly different functional forms such as

$$C_p = A^*\epsilon^{-\alpha^*}[1 + D^*\epsilon^{x^*}] + B^*, \qquad (5.16b)$$

which also include singular correction terms that vary as a power of ϵ. The values of the amplitudes and exponents in Eqs. (5.16a) and (5.16b) which can be obtained from a fit to a given set of data will not differ much. When α and α' are not fixed at a predetermined value, we prefer Eq. (5.16a), because A and B are analytic functions of α, whereas A^* and B^* are singular for $\alpha^* = 0$. Such singularities are inconvenient in an iterative nonlinear least-squares problem. We have ascertained, however, that x^* is about equal to $x - 0.1$ for the range of α or α^* pertinent to our data, and that α and α^* differ insignificantly from each other.

Equation (5.16a) without any additional restrictions has many highly correlated parameters, and therefore it yields sufficiently large statistical errors for the parameters to accommodate most theoretical predictions. This is true even when it is fitted to data with a precision of 0.1% over two decades in $|\epsilon|$ with all $|\epsilon| \leq 3\times10^{-3}$. We will first compare Eq. (5.16a) with the experiment with a minimum number of restrictions upon the parameters. Fitting it to the data at one particular pressure, we were not able to simply least-squares adjust all the parameters because the high correlation between them, in conjunction with the available numerical precision, prevented convergence of the iterative nonlinear least-squares fit. We were more successful when x was held constant at a predetermined value, and Fig. 23 shows α and α' as a function of x for the 25.86-bar data. The error bars do not, of course, include any correlation of α or α' with x. It is apparent that α and α' are not very sensitive to the choice of x. For $x \lesssim 1$, the results are consistent with $\alpha = \alpha'$. Therefore, we have next assumed that Eq. (5.4) is indeed valid, and analyzed the results at each P with the constraints $\alpha = \alpha'$ and $x = x'$. During this analysis, x was still held constant, and $\alpha = \alpha'$ was determined at each pressure for several $x = x'$. The results are shown in Fig. 24. In this case, the solid circles indicate that the estimate of the variance based on the fit was sufficiently small that the fit may be regarded as satisfactory. The values of α represented by open circles correspond to unsatisfactory fits, implying that the assumed value of x was outside an acceptable range. The data indicate that generally any value of x between 0.5 and 0.9 is acceptable. Over this range of x, the data do not indicate any pressure dependence of α and α', and one has approximately

$$-0.04 \lesssim \alpha = \alpha' \lesssim 0.02, \qquad (5.17a)$$

$$0.5 \lesssim x = x' \lesssim 0.9. \qquad (5.17b)$$

Equation (5.17a) permits a rather large range of values for α and α'. This range becomes somewhat narrower if the value of x and x' is restricted. Recent calculations[40] indicate that x probably has a value near 0.5. If the additional constraint $x = x'$

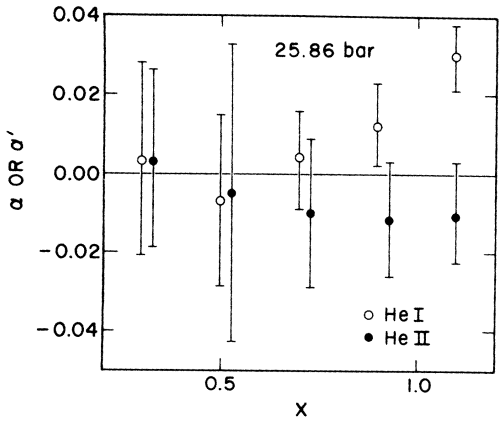

FIG. 23. Leading exponents α and α', determined independently of each other, using Eq. (5.16a), as a function of the fixed value x of the exponent for the correction term. The results are for 25.86 bar.

$= 0.5$ is imposed, the data yield

$$\alpha = \alpha' \cong -0.02 \pm 0.02 \quad \text{if } x = x' = 0.5 . \qquad (5.18)$$

The result Eq. (5.18) is of course dependent upon the assumption $\alpha = \alpha'$. Also, consistent with the data, α and α' are assumed independent of P. The result Eq. (5.18) is in remarkably good agreement with the calculations by Wilson[38] and Brézin *et al.*,[39] which to second order in $4-d$ yield $\alpha = \alpha' = -\frac{1}{50}$ for a system of dimensionality $d = 3$ whose order parameter has two degrees of freedom (see also Sec. VH).

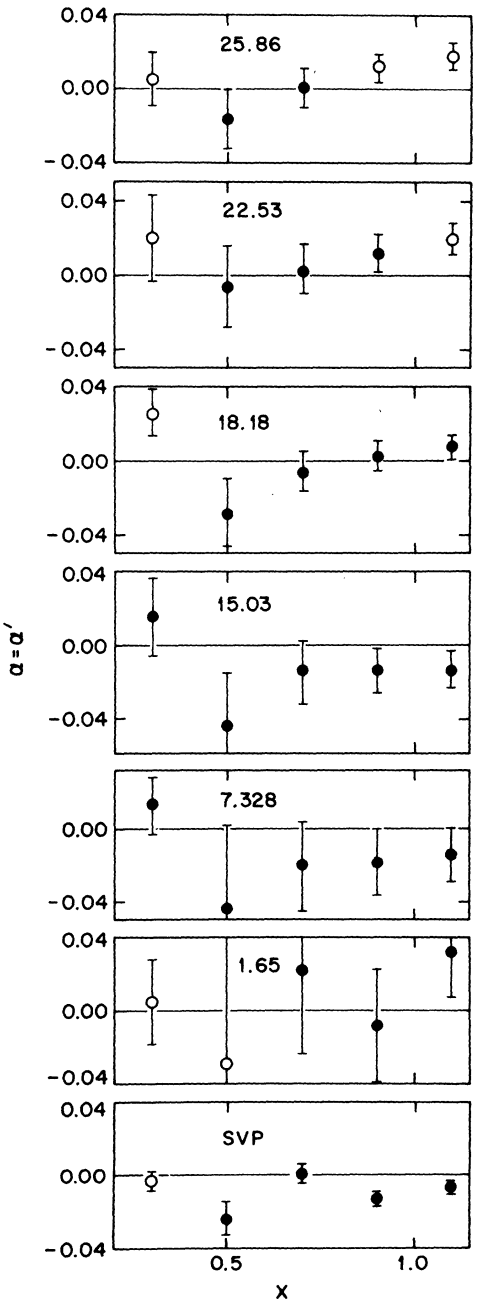

FIG. 24. Leading exponent α or α', determined under the constraint $\alpha = \alpha'$, using Eq. (5.16a), as a function of the fixed value $x = x'$ of the exponent for the correction term. The number near the top of each block is the pressure in bars.

There have been several other recent, usually more empirical and often less specific, suggestions about the form of higher-order singular contributions to the equation of state.[48-53] Although they do not all make explicit predictions about the specific heat, it is likely that the various approaches would all yield values of x which fall in the range of Eq. (5.17b). However, recent results for the superfluid density ρ_s (Ref. 54) have also revealed the existence of singular correction terms. It appears[40,49] that the correction exponent for this variable should be essentially the same as the one for C_p, and the ρ_s results yield $0.4 \lesssim x \lesssim 0.6$. Therefore the two sets of data considered together permit only values of x near $\frac{1}{2}$. This is in agreement with the estimate by Wegner,[40] but tends to exclude some of the other approaches which yield larger values of x.

Let us proceed further by investigating the behavior of the amplitude ratio A/A' over a reasonable range of x and α. We should do this by assuming $\alpha = \alpha'$ and $x = x'$. With these restrictions it is possible to obtain precise values of A/A' as a function of x and α. These results are shown in Fig. 25 for $P = 25.86$ bar. Again only data with $|\epsilon| \leq 3 \times 10^{-3}$ were used in the analysis. It can be seen that A/A' at constant x is virtually independent of α for $0.00 \leq \alpha = \alpha' \leq 0.08$ and at constant α only mildly dependent upon x. Even for large x, A/A' tends towards a limit which is larger than 1.

As x becomes large, $|D|$ and $|D'|$ become large also. As an example of this, D is shown in Fig. 26 as a function of x for the results at 25.86 bar for three values of α. Since D and D' are pure

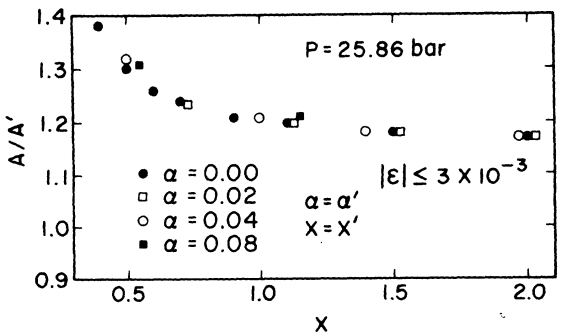

FIG. 25. The amplitude ratio A/A', determined by fitting the results at 25.86 bar to Eq. (5.16a) with fixed α and x (or α' and x') for four values of $\alpha = \alpha'$ as a function of $x = x'$.

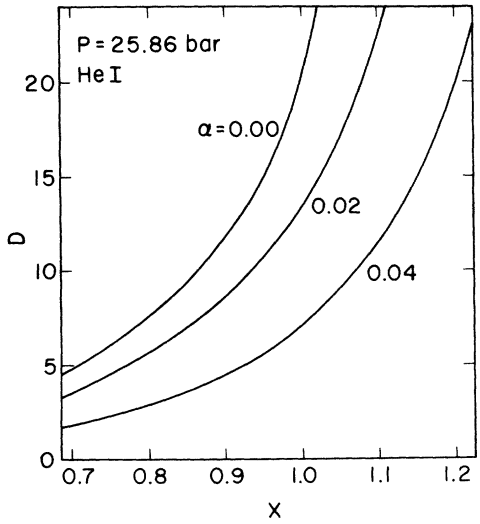

FIG. 26. Amplitude D of the correction term in Eq. (5.16a) at 25.86 bar as a function of x for several α.

numbers, one might expect them to be of order unity; therefore it is unlikely that $x \gtrsim 1.0$ where $D \gtrsim 10$. This conclusion is of course in agreement with the earlier one that $0.5 \leq x \leq 0.9$.

Since A/A' is independent of α, we can compare the results for A/A' in Fig. 25 with the previous estimates of A_0/A_0' which assumed $\alpha = \alpha' = 0$ and which were shown in Fig. 22. The results in Fig. 25 are consistent with those in Fig. 22 for $x \gtrsim 0.7$. If indeed $x \gtrsim 0.7$, then A/A' can be expected at all pressures to be equal to the A_0/A_0' in Fig. 22 within the error bars which are shown. If $x < 0.7$, A/A' may be somewhat larger; but the pressure dependence in Fig. 22 would still exist if x is independent of P.

The result Eq. (5.17a) permits $\alpha = \alpha' \neq 0$ and independent of P, and therefore the scaling prediction $A_0/A_0' = 1$ need not be applicable. The results show that $A/A' > 1$. This inequality, in conjunction with $\alpha = \alpha' \geq 0$, implies that for sufficiently small ϵ, C_p above T_λ is larger than C_p below T_λ at the same $|\epsilon|$. This can be seen readily from Fig. 20, where a linear extrapolation to smaller $|\epsilon|$ will cross zero and yield a positive $C_p^I(|\epsilon|) - C_p^{II}(|\epsilon|)$. Although there appears to be no thermodynamic or scaling argument which is violated by such a behavior, it is most unexpected, and no detailed equation of state with this property has as yet been proposed.

The result Eq. (5.17a) of course also permits $\alpha = \alpha' < 0$. In that case, C_p is finite at T_λ. The amplitude ratio A_0/A_0' shown in Fig. 22 would still be representative of A/A'. For negative α and α', $A/A' > 1$ is not so unusual, and would result from many equations of state[5,43] which have been considered in the past. But again, the data yield an A/A' which depends upon the pressure in accordance with Fig. 22. One would still have expected A/A' to be independent of the pressure, since the equation of state of Brézin *et al.*[39] contains no relevant pressure-dependent parameters and yields an A/A' which depends only on the dimensionality of the system which is three, and on the number of degrees of freedom of the order parameter which is two. An explicit calculation of A/A' based on this equation would be of interest.

Of the possible interpretations of the data which have been discussed, the one represented by Eq. (5.18) comes closest to being consistent with theo-

TABLE XI. Parameters of Eq. (5.16b) with the constraints $\alpha^* = \alpha^{*\prime}$ and $x^* = x^{*\prime} = \frac{1}{2}$, for $\alpha^* = \alpha^{*\prime} = -0.02$ and $\alpha^* = \alpha^{*\prime} = -0.04$. $R = 8.314$ J mole^{-1}K^{-1} was used where needed to make the parameters dimensionless.

P(bar)	$\alpha^{*\prime}A^{*\prime}/R$	$A^*/A^{*\prime}$	$B^{*\prime}/R$	$(B^* - B^{*\prime})/R$	$-D^*$	$-D^{*\prime}$
		$\alpha^* = \alpha^{*\prime} = -0.02$, $x^{*\prime} = 0.5$				
0.05	0.735	1.065 ± 0.009	38.08	−0.55 ± 0.26	0.07	0.00
1.65	0.725	1.096 ± 0.044	37.50	+0.38 ± 1.27	0.09	0.03
7.33	0.704	1.062 ± 0.024	36.10	−0.65 ± 0.67	0.09	0.07
15.03	0.667	1.059 ± 0.023	34.09	−0.73 ± 0.60	0.06	0.09
18.18	0.633	1.184 ± 0.022	32.43	+2.48 ± 0.51	0.18	0.08
22.53	0.586	1.334 ± 0.028	30.20	+5.80 ± 0.57	0.29	0.07
25.86	0.623	1.236 ± 0.021	31.75	+3.66 ± 0.47	0.24	0.12
		$\alpha^* = \alpha^{*\prime} = -0.04$, $x^* = x^{*\prime} = 0.5$				
0.05	0.895	1.065 ± 0.010	21.43	−1.54 ± 0.14	0.25	0.14
1.65	0.878	1.084 ± 0.044	21.30	−1.21 ± 0.64	0.26	0.18
7.33	0.849	1.076 ± 0.024	20.17	−1.32 ± 0.32	0.31	0.24
15.03	0.817	1.061 ± 0.022	18.96	−1.49 ± 0.29	0.27	0.32
18.18	0.773	1.179 ± 0.023	19.51	+0.05 ± 0.26	0.45	0.29
22.53	0.717	1.341 ± 0.031	20.12	+1.89 ± 0.31	0.71	0.27
25.86	0.760	1.229 ± 0.022	19.56	+0.56 ± 0.25	0.56	0.35

ry. Of course, the theoretical result Eq. (5.5) and the data exclude a zero exponent because $A/A' \neq 1$, and therefore theory and experiment jointly yield

$$-0.04 \lesssim \alpha = \alpha' < 0. \qquad (5.18')$$

We present in Table XI the parameters obtained by fitting Eq. (5.16b) to the data, with the two fixed values of -0.02 and -0.04 for $\alpha^* = \alpha^{*\prime}$. Here the correction term exponents were fixed at $x^* = x^{*\prime} = \frac{1}{2}$. Again it is evident that $A^*/A^{*\prime}$ is independent of the leading exponent, but dependent upon P. For $\alpha^* = \alpha^{*\prime} = -0.02$, $B^* - B^{*\prime}$ is zero within error for $P \lesssim 15$ bar, implying a continuous C_p at T_λ. This is consistent with Eq. (5.9). For larger P, where $A^*/A^{*\prime}$ is dependent upon P, $B^* - B^{*\prime}$ is no longer zero if $\alpha^* = \alpha^{*\prime} = -0.02$. It is clear from the results in Table XI that a continuous C_p which agrees with Eq. (5.9) can be obtained from the data only if $\alpha^* = \alpha^{*\prime}$ depends upon P and varies from near -0.02 to near -0.04 as P changes from 0 to 26 bar. For α^* and $\alpha^{*\prime}$ between -0.02 and -0.04, the finite C_p at T_λ is predicted to be in the range $20-40R$ (R is the gas constant), which is a factor of 2–4 larger than the largest measured C_p.

F. Heat Capacity near the Superfluid Transition in He^3-He^4 Mixtures

In Secs. V C–V E it was demonstrated that, even when reasonable latitude is permitted in the form of singular higher-order terms which are included in the data analysis, it is difficult to escape the conclusion that there is an asymmetry about T_λ in C_p which is not fully explained by that part of the theory which pertains to the asymptotic behavior. This asymmetry is reflected for instance in the unusual ϵ and P dependence of ΔC_p which is shown in Fig. 20. Although we were able to obtain agreement with theory to a large extent essentially by attributing the asymmetry to different amplitudes for the correction terms above and below T_λ, and to a pressure-dependent amplitude ratio for the leading term, we would now like to inquire whether its existence is supported by an asymmetry in measurements of the appropriate response function for He^3-He^4 mixtures. For that system there exist rather precise data by Gasparini and Moldover[55,56] for the heat capacity C_{xp} at constant pressure equal to the saturated vapor pressure, and constant He^3 concentration. It is easy to show, however, on purely thermodynamic grounds that C_{xp} in general is finite at T_λ, except at zero He^3 concentration, where it is equal to C_p for the pure system and may diverge. In this case C_{xp} occupies a position rather similar to that of C_v in the pure system, and it has been possible to calculate[55,56] reasonably reliably at least at the lesser concentrations the heat capacity at constant chemical potential difference

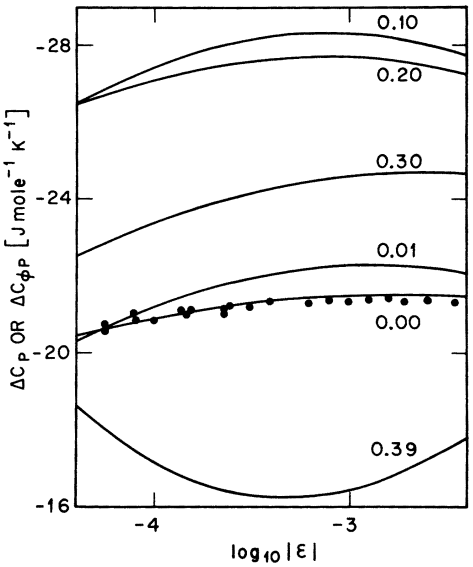

FIG. 27. Difference $\Delta C_{\Phi P}$ between $C_{\Phi P}$ for He I and $C_{\Phi P}$ for He II along lines of constant chemical potential difference Φ for He^3-He^4 mixtures as a function of $\log_{10}|\epsilon|$. The numbers in the figure are the He^3 mole fraction at T_λ. The solid lines are calculated from the power laws given in Ref. 56. The individual points are for pure He^4 from Ref. 1, and are some of those shown in Fig. 20.

$C_{\Phi p}$. $C_{\Phi p}$ is permitted by thermodynamics to diverge at all concentrations. Indeed, when data for $C_{\Phi p}$ were fitted to a power law like Eq. (5.1), values of α and α' near zero were obtained.[56] We show as solid lines in Fig. 27 the differences $\Delta C_{\Phi p}$ between the power laws above and below T_λ which were obtained[56] from the data by a least-squares method. It is immediately apparent for concentrations up to a He^3 mole fraction of 0.3 that $\Delta C_{\Phi p}$ is rather similar in its ϵ dependence to the ΔC_p shown for pure He^4 in Fig. 20. The result for zero concentration can of course be compared directly with the vapor-pressure measurements in pure He^4. Some of the He^4 SVP results[1,2] which were shown in Fig. 20 are repeated here as individual points, and agree nearly perfectly with the smoothed $\Delta C_{\Phi p}$ for $x = 0$ from Refs. 55 and 56. At $x = 0.39$, the calculation of $C_{\Phi p}$ from C_{xp} is not very precise because the difference is large, and the apparently different behavior of $\Delta C_{\Phi p}$ at this concentration may not be real. We conclude that the measured C_{xp} in the mixtures fully support the existence of the asymmetry about T_λ which we have discussed for the pure system.

G. Comparison with Thermal Conductivity of He I and the Superfluid Density of He II

Although C_p could be represented well by pure power laws (see Sec. IV C and Fig. 18), it has be-

come apparent from the analysis of C_p that it is not possible to obtain agreement with scaling unless singular higher-order contributions are permitted. Specific theoretical predictions pertaining to such higher-order terms have become available only very recently[40] but the existence of such terms at least in some properties near T_λ has been evident from experiment for some time. They were revealed first by measurements of the thermal conductivity λ of He I near T_λ under pressure.[6] These results could not be fitted at all by a pure power law, or by a power law with logarithmic corrections suggested by theory,[31] even when data were restricted to $\epsilon \lesssim 10^{-4}$. Recent high precision measurements of the superfluid density ρ_s (Ref. 54) have revealed that singular higher-order terms exist also in this parameter. As in the case of λ, a statistically satisfactory fit of the ρ_s measurements to a pure power law could not be obtained and the existence of singular correction terms was established on the basis of the data alone. The results for ρ_s were fitted to the equation

$$\rho_s/\rho = k\epsilon^{\zeta}[1 + a\epsilon^{y}], \tag{5.19}$$

with k and a analytic functions of P. They yielded[54]

$$0.66 \lesssim \zeta \lesssim 0.68 \tag{5.20}$$

as an estimate of the asymptotic exponent ζ. This result can be compared with the result Eq. (5.17a) which pertains to C_p, and which is also based on the assumption of power-law correction terms to the asymptotic behavior. Equation (5.17) yields

$$0.660 \leq \tfrac{1}{3}(2 - \alpha') \leq 0.680. \tag{5.21}$$

This agrees well with the result Eq. (5.20) and the scaling law Eq. (5.7). The asymptotic behavior of λ has been compared elsewhere[6] with that of C_p, and does not appear to agree with the predictions of dynamic scaling[31]; but the possible existence of logarithmic terms in the theory in addition to higher-order singular power-law terms make the interpretation of the data extremely difficult. A more thorough analysis still needs to be done. The problem would be eased considerably by specific predictions for the exponent of higher-order contribution to λ.

Since C_p, λ, and ρ_s all seem to contain singular corrections to the leading power-law contribution, one might enquire whether the experimental results for the correction exponents are consistent with each other and with theoretical predictions. For λ, there are no specific predictions of the correction terms at this time. However, it appears that the exponents x and y in Eqs. (5.16a) and (5.19) for C_p and ρ_s should be approximately equal to each other,[40,49] and that their value should be near 0.5.[40] The result Eq. (5.17b) agrees with this prediction, but leaves so much latitude in x that the comparison does not constitute a very severe test of the theory. In the case of ρ_s, the exponent y of the correction term in Eq. (5.19) may have a value somewhere between 0.4 and 0.6. This also agrees with the theoretical value. Somewhat less latitude than in x is permitted by the data in the value of y; and if we expect $x \cong y$ as suggested by theory, then only values near 0.5, say

$$x \cong y \cong 0.5 \pm 0.1, \tag{5.22}$$

would be permitted by the two sets of measurements. This result is in good agreement with the calculation.[40]

The constant $y = 0.5$ which is suggested by theory and which was used in Sec. E for C_p [see Eq. (5.18)] can also be adopted in the analysis of ρ_s; but most of the uncertainty in ζ is attributable to systematic errors, and an independent value for y does not reduce the error of ζ appreciably.[54] Thus, even for $y \equiv \frac{1}{2}$ the result Eq. (5.20) pertains. However, if the scaling predictions Eqs. (5.4) and (5.5) are assumed valid, then the result $A/A' > 1$ and the result Eq. (5.18) imply $\alpha = \alpha' < 0$. Thus, Eq. (5.7) and Eq. (5.20) yield

$$2/3 < \zeta \leq 0.68. \tag{5.23}$$

The best value of α and α' given by Eq. (5.18) yields $\frac{1}{3}(2 - \alpha') = 0.673$. This is in particularly good agreement with the value[54] $\zeta = 0.674$ obtained by fitting the ρ_s results at vapor pressure, where contributions from correction terms appear small, to a pure power law. We note that at vapor pressure and $T < T_\lambda$ a fit of C_p to a pure power law[1,2] yields $\alpha' = -0.02$. This agrees with the best estimate Eq. (5.18) for all pressures and suggests that at SVP contributions from correction terms are small also for C_p below T_λ.

H. Comparison with Other Systems

The analysis in Secs. V E and V G revealed that only a slightly negative value of α and α' is consistent with the measurements and most of the theoretical predictions (of course even then the problem of the pressure-dependent amplitude ratio remains). We now wish to examine whether the result $0 > \alpha = \alpha' \cong -0.02$ is consistent with experimental measurements for the heat capacity near other critical points.

According to the recent theoretical work by Wilson,[38,39] the exponents are given as an expansion in $4 - d$, where d is the dimensionality (i.e., $d = 3$) of the system. The coefficients in this expansion are functions only of the number of degrees of

freedom n of the order parameter.[56a] We would thus expect $\alpha = \alpha'$ to be a smoothly varying function of n. Therefore, we have collected in Fig. 28 what appear to be the best available experimental estimates of $\alpha = \alpha'$ for different types of systems with $n = 1$, 2, and 3.

For $n = 1$, measurements near liquid-gas critical points, order-disorder transitions, and transitions in Ising magnets pertain. Of these, the heat capacity near the critical point in CO_2 (Ref. 42) and in He^3 (Ref. 57) yield perhaps the most reliable exponents, and result in $\alpha = \alpha' \cong \frac{1}{8}$. For $n = 2$, the superfluid transition discussed in this paper yields $\alpha = \alpha' \cong -0.02$. For $n = 3$, Heisenberg systems pertain, and the most reliable experimental results have been obtained for the antiferromagnetic transition in $RbMnF_3$. These data yielded[58] $\alpha = \alpha' = -0.14 \pm 0.01$. There are no other values of n for which experiments are possible, but $n = \infty$ corresponds to the exactly soluble spherical model[59] which has $\alpha = \alpha' = -1$. The solid line in Fig. 28 is drawn through the experimental data, and continues smoothly for small $1/n$ to the value -1 for α of the spherical model. Near $1/n = 0$, this line is drawn with the limiting slope $32/\pi^2$ which is predicted by theory in three dimensions from an expansion of α in $1/n$.[60] It is evident that the theoretical results for large n and the experimental data for $n = 1$, 2, and 3 yield a smooth dependence of α upon n. In particular the very slightly negative α for $n = 2$, which was obtained in this work, is quite consistent with the known theoretical and experimental results for other values of n.

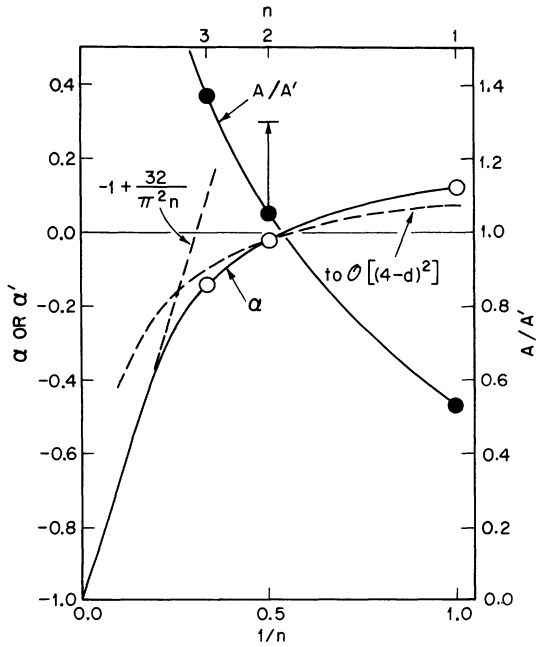

FIG. 28. Dependence of α and α' upon the number of degrees of freedom of the order parameter. The open circles represent the experimental results for liquid-gas critical points ($n = 1$), for the superfluid transition ($n = 2$), and for Heisenberg systems ($n = 3$). The spherical model has $1/n = 0$, and yields $\alpha = \alpha' = -1$. See Sec. V H for details. Also shown, as solid circles, are the experimental amplitude ratios A/A' for $n = 1$, 2, and 3.

The dashed curve in Fig. 28 is an estimate to second order in $4 - d$ of α which was obtained[61] from the expansion by Wilson[38] of exponents in the dimensionality. This estimate also agrees quite well with the experimental values.

Instead of the exponent, one could also compare the amplitude ratio A/A' that is obtained from measurements on systems with different values of n. As for α and α', it is expected that A/A' is a function only of d and n.[39] Therefore, the experimental A/A' for the liquid-gas critical point,[42] for the superfluid transition at pressures less than 15 bar, and for $RbMnF_3$ (Ref. 58) are shown as well in Fig. 28. As we saw for the exponents, the values of A/A' also fall on a smooth curve. This curve yields $A/A' = 1$ at the value of $1/n$ where $\alpha = \alpha' = 0$; and therefore the scaling prediction Eq. (5.5) is consistent with experiment. The larger values of A/A' obtained for the superfluid transition at the higher pressures are indicated by the arrow on the point for $1/n = 0.5$. They could also be connected with the results for other n by a smooth function; but the curve through the large A/A' for $n = 2$ and through the results for $n = 1$ and $n = 3$ would not yield $A/A' = 1$ when $\alpha = \alpha' = 0$, and would therefore be inconsistent with scaling.

VI. SUMMARY AND CONCLUSIONS

In this paper we have described modifications which were made to previously discussed apparatus and procedures[1] for the measurement of thermodynamic properties near the superfluid transition. With these changes, the transition was investigated as a function of pressure by measuring the heat capacity at constant volume C_v and the pressure coefficient $(\partial P/\partial T)_v$ along six isochores. The results, together with those at vapor pressure,[1,2] provide a complete thermodynamic description of the transition, and were used to derive the heat capacity at constant pressure C_p, the isobaric thermal-expansion coefficient α, the isothermal compressibility κ, the ratio γ of C_p to C_v, and the isentropic sound velocity u, all along isobars. The results span approximately the range $-10^{-2} \leq T - T_\lambda \leq 10^{-2}$ K. In addition, new values of the temperature derivative of the volume and the entropy along the λ line were obtained from the measurements.

The results for the heat capacity at constant pressure C_p along isobars were analyzed in terms of power laws, and the resulting parameters were

compared with theoretical predictions.[3,4,38-41,59,60] We summarize the results as follows.

(a) When the data with $\epsilon \equiv |T/T_\lambda - 1| \leq 1.6\times10^{-3}$ were fitted to a pure power law, the resulting exponents α and α' above and below T_λ within their statistical and systematic errors were not equal to each other at some pressures. From this it follows either that the theoretical prediction[3,4] $\alpha = \alpha'$ for the asymptotic exponents is not valid, or that there are large contributions to C_p even for small ϵ which are not attributable to the asymptotic behavior.

(b) Since pure power laws in conjunction with the data are incompatible with theory, the results were next fitted to power laws with singular correction terms. The higher-order contributions were also written in the form of power laws. The high statistical correlation between the larger number of parameters in this analysis resulted in larger errors for α and α'. Independent of pressure, $-0.04 \leq \alpha = \alpha' \leq 0.02$ was obtained. Within these larger errors this result is consistent with the theoretical prediction[3,4] $\alpha = \alpha'$ and with universality.[10]

(c) When the exponent for the correction term was fixed at the recently predicted[40] theoretical value of 0.5, the permitted range of α and α' was restricted to $-0.04 \leq \alpha = \alpha' \leq 0.00$.

(d) The ratio A/A' of the amplitude above and below T_λ of the leading contribution to C_p was insensitive to the value chosen for α, provided the constraint $\alpha = \alpha'$ was imposed. For all α, we found $A/A' > 1$. Therefore, the data agree with theory[3,4] only if $\alpha = \alpha' \neq 0$; for if $\alpha = \alpha' = 0$, then scaling requires $A/A' = 1$.

(e) If the correction exponent is fixed at a value near 0.5 as theoretically predicted,[40] then the measured amplitude ratio $A/A' > 1$, the scaling law[3,4] $A/A' = 1$ if $\alpha = \alpha' = 0$, and the result of (c) above permit only negative values of α and α'. Thus, we obtain agreement with theory only if C_p is finite at T_λ.

(f) The permitted range $-0.04 \leq \alpha = \alpha' < 0$ is in good agreement at all pressures with recent measurements[54] of the exponent ζ for the superfluid density ρ_s and the scaling prediction[3,4,41] $\zeta = \frac{1}{3}(2 - \alpha')$. The values permitted for α and ζ also agree well with the result $\alpha = -1/50$ and $\zeta = 0.673$ obtained from recent calculations.[38,39]

(g) Regardless of what choice is made for α and α' within the permitted range, the data show that the amplitude ratio A/A' depends upon the pressure. Although explicit calculations for A/A' have not been made, no pressure dependence is expected for this quantity.

(h) Although the measured C_p can be fit well by a pure power law and does not by itself provide evidence for the existence of singular correction terms, such higher-order contributions have been observed more directly for small ϵ in the thermal conductivity λ of He I (Ref. 6) and in the superfluid density ρ_s of He II.[54] Therefore, invoking such terms in order to obtain agreement for the leading exponents with theory is not unreasonable.

(i) The finite value of C_p at T_λ which is obtained from the data with a negative $\alpha = \alpha'$ is only 2–4 times larger than the largest measured C_p. If $\alpha = \alpha' = -0.02$, then C_p may be continuous only for $P \lesssim 15$ bar, and will be discontinuous for larger P.

(j) A very slightly negative exponent is consistent with experimental and theoretical results for other systems and a smooth dependence of exponents upon the number of degrees of freedom of the order parameter.

We summarize our results by stating that nearly full agreement between our data and existing theoretical predictions[3,4,38-41] can be obtained only if singular higher-order contributions to C_p are permitted, and if C_p is finite at T_λ (i.e., $\alpha = \alpha' < 0$). Even in this case, the ratio A/A' of the leading amplitudes depends upon the pressure. This pressure dependence appears contrary to theory. In addition, the data are not consistent with a continuous C_p at all pressures if α and α' are universal.

VII. ACKNOWLEDGMENT

I am most grateful to P. C. Hohenberg for countless stimulating discussions throughout the duration of this work.

[1]G. Ahlers, Phys. Rev. A 3, 696 (1971).
[2]G. Ahlers, Phys. Rev. Lett. 23, 464 (1969).
[3]B. Widom, J. Chem. Phys. 43, 3892 (1965); J. Chem. Phys. 43, 3898 (1965).
[4]L. P. Kadanoff, Physics 2, 263 (1966).
[5]R. B. Griffiths, Phys. Rev. 158, 176 (1967).
[6]G. Ahlers, in *Proceedings of the Twelfth International Conference on Low Temperature Physics*, edited by E. Kanda (Academic, Japan, 1971), p. 21.
[7]G. Ahlers, Phys. Lett. 39A, 335 (1972).
[8]G. Ahlers, Bull. Am. Phys. Soc. 17, 277 (1972).
[9]The most detailed evidence for the "sharpness" of the superfluid transition under pressure consists of thermal conductivity measurements [Ref. 6 and G. Ahlers (unpublished)] which show that except for gravity effects any "rounding" is confined to $|\epsilon| < 10^{-7}$ at all pressures.
[10]See, for instance, L. P. Kadanoff, *Critical Phenomena, Proceedings of the International School "Enrico*

Fermi", edited by M. E. Green (Academic, New York, 1971); or R. B. Griffiths, Phys. Rev. Lett. 24, 1479 (1970).

[11]For the LPTI gauge the same type of oscillatory component of the gauge reading as a function of pressure observed for tube serial No. 2564, gauge serial No. 1344 (see Ref. 1, Fig. 4) was again observed.

[12]A very constant pressure was obtained for this purpose by filling the sample container (81 cm^3) with liquid He^4 to the desired pressure, and holding its temperature constant to $\pm 10^{-6}$ K.

[13]G. Ahlers, Phys. Rev. Lett. 24, 1333 (1970).

[14]The auxiliary capillary was necessary for cooling of He^3-He^4 mixtures (Ref. 13). With mixtures, He^3 enrichment of the gas in the main capillary due to superfluid film flow resulted in loss of superfluidity. Further cooling then became impossible, and temperatures below about 4 K could not be reached without the auxiliary capillary.

[15]Precision measurements of the thermal conductivity of He I were made with relatively high power densities, and have been reported briefly in Ref. 6.

[16]G. Ahlers, Phys. Rev. 171, 275 (1968).

[17]H. A. Kierstead, Phys. Rev. 162, 153 (1972).

[18]M. J. Buckingham and W. M. Fairbank, in *Progress in Low Temperature Physics*, edited by C. J. Gorter (North-Holland, Amsterdam, 1961), Vol. III, p. 80.

[19]M. E. Fisher, J. Math. Phys. 5, 944 (1964); Phys. Rev. 136, A1599 (1964).

[20]O. V. Lounasmaa and E. Kojo, Ann. Acad. Sci. Fenn. AVI, No. 36 (1959).

[20a]T. H. McCoy and E. H. Graf, Phys. Lett. 38A, 287 (1972).

[21]H. A. Kierstead, Phys. Rev. 153, 258 (1967); Phys. Rev. 160, 262(E) (1967).

[22]A. B. Pippard, Phil. Mag. 1, 473 (1956); and A. B. Pippard, *The Elements of Classical Thermodynamics* (Cambridge U. P., Cambridge, England, 1957), Chap. IX.

[23]O. K. Rice, J. Chem. Phys. 22, 1534 (1954).

[24]M. Barmatz and I. Rudnick, Phys. Rev. 170, 224 (1968).

[25]G. Ahlers, Phys. Rev. 182, 352 (1969).

[26]R. W. Hill and O. V. Lounasmaa, Phil. Mag. 2, 143 (1957).

[27]C. G. Waterfield, J. K. Hoffer, and N. E. Phillips (unpublished).

[28]O. V. Lounasmaa, Cryogenics 1, 1 (1961).

[29]G. Ahlers, J. Low Temp. Phys. 7, 361 (1972).

[30]O. V. Lounasmaa, Phys. Rev. 130, 847 (1963).

[31]B. I. Halperin and P. C. Hohenberg, Phys. Rev. 177, 952 (1969).

[32]E. R. Grilly, Phys. Rev. 149, 97 (1966).

[33]D. L. Elwell and H. Meyer, Phys. Rev. 164, 245 (1967).

[34]D. L. Elwell, Ph.D. thesis (Dept. of Physics, Duke University, 1967) (unpublished).

[35]C. J. Palin, W. F. Vinen, and J. M. Vaughan, J. Phys. C: Solid State Phys. 5, L139 (1972).

[36]W. F. Vinen, C. J. Palin, and J. M. Vaughan, in Proceedings of the 13th International Conference on Low Temperature Physics, Boulder, Colorado (unpublished).

[37]G. Winterling, F. S. Holmes, and T. J. Greytak, in Proceedings of the 13th International Conference on Low Temperature Physics, Boulder, Colorado (unpublished).

[38]K. G. Wilson, Phys. Rev. Lett. 28, 548 (1972).

[39]E. Brézin, D. J. Wallace, and K. G. Wilson, Phys. Rev. Lett. 29, 591 (1972); Phys. Rev. B 7, 232 (1973).

[40]F. J. Wegner, Phys. Rev. B 5, 4529 (1972).

[41]B. D. Josephson, Phys. Lett. 21, 608 (1966).

[42]J. A. Lipa, C. Edwards, and M. J. Buckingham, Phys. Rev. Lett. 25, 1086 (1970).

[43]P. Schofield, J. D. Litster, and J. T. Ho, Phys. Rev. Lett. 23, 1098 (1969).

[44]B. D. Josephson, J. Phys. C: Solid State Phys. 2, 1113 (1969).

[45]P. Schofield, Phys. Rev. Lett. 22, 606 (1969).

[46]P. Szépfalusy, Phys. Lett. 32A, 127 (1970).

[47]M. E. Fisher, Phys. Rev. 180, 594 (1969).

[48]C. Domb and D. S. Gaunt, J. Phys. (Paris) 32, C1-344 (1971).

[49]M. S. Green, M. J. Cooper, and J. M. H. Levelt Sengers, Phys. Rev. Lett. 26, 492 (1971).

[50]D. Stauffer and C. J. Kiang, Phys. Rev. Lett. 27, 1783 (1971).

[51]N. D. Mermin and J. J. Rehr, Phys. Rev. A 4, 2408 (1971).

[52]M. J. Cooper, Phys. Rev. A 5, 318 (1972).

[53]F. J. Cook and M. S. Green (unpublished).

[54]D. S. Greywall and G. Ahlers, Phys. Rev. Lett. 28, 1251 (1972); Phys. Rev. A 7, 2145 (1973).

[55]F. M. Gasparini and M. R. Moldover, Phys. Rev. Lett. 23, 749 (1969).

[56]F. M. Gasparini, Ph.D. thesis (Dept. of Physics, University of Minnesota, 1970) (unpublished).

[56a]Strictly, this is correct only for systems with short-range interactions. See A. Aharony and M. E. Fisher, Phys. Rev. Lett. 30, 559 (1973).

[57]G. R. Brown and H. Meyer, Phys. Rev. A 6, 364 (1972).

[58]A. Kornblit, G. Ahlers, and E. Buehler Phys. Lett. (to be published); A. Kornblit and G. Ahlers (to be published).

[59]See, for instance, H. E. Stanley, *Introduction to Phase Transitions and Critical Phenomena* (Oxford U. P., New York, 1971).

[60]S. Ma, Phys. Rev. Lett. 29, 1311 (1972); and E. Brézin and D. J. Wallace, Phys. Rev. B7, 1967 (1973).

[61]We used the expansion in $(4-d)$ for γ and η from Ref. 38, and the scaling relation $\alpha = 2 - d\gamma/(2-\eta)$, all to $\mathcal{O}[(4-d)^2]$.